The Abdus Salam
International Centre for Theoretical Physics

United Nations
Educational, Scientific
and Cultural Organization

International Atomic
Energy Agency

World Year of PHYSICS 2005

SMR.1670 - 26

INTRODUCTION TO MICROFLUIDICS

8 - 26 August 2005

Two-phase Micro-flow

Vesicle Orientation and Dynamics in Shear Flow

V. Steinberg
Weizmann Institute of Science, Israel

Two-phase micro-flow

(bubble generation, formation, emulsion in micro-channel, drop as a chemical reactor, dynamics and statistics of vesicles in shear flow)

Lecture 6

V. Steinberg

Summer School in Microfluidics,
August 8-26, 2005, ICTP, Trieste, Italy

WEIZMANN
INSTITUTE
OF SCIENCE

Introduction

Relevant parameters for the problem: ***Re*** and Weber, or capillary number, ***Ca***

The main questions:

(i) Drop formation, coalescence, and break-up
(ii) Drop movement in small channels
(iii) Internal mixing in drops

Main applications:

- drops as actuators for pumping a primary flow or driving mixing flows
- drops as individual “chemical reactors”
- formation of emulsion with a controlled and uniform drop size

From physical point of view it is rather interesting system since shows unexpectedly rich pattern behavior

Parameters of the problem and numbers

$Ca = \eta V / \sigma$ -the capillary number

σ -surface tension

Characteristic numbers for water with surfactant:

$$\eta \approx 10^{-2}\, gcm/s; \sigma \approx 30 g/s^2$$

$$V \approx 1-10 cm/s; Ca \approx 10^{-3} - 10^{-2}$$

Gravitational effects are negligible: $\Delta \rho g h^2 / \sigma \approx 10^{-4}$

Strain rate $\dot{\gamma} \approx \frac{V}{h} \propto 10^3 - 10^4 s^{-1}$ is usually large to result in non-Newtonian effects if suspended deformable objects are present (drops, macromolecules, surfactant meso-phases, etc) with

$Wi = \dot{\gamma} \cdot \tau$

τ as the relaxation time

Perfectly monodisperse micro-bubbling by capillary flow focusing

A. Ganan-Calvo&J.Gordillo, PRL **87**, 274501 (2001)

Self-excited break-up phenomenon of micro-jet that leads to formation of monodisperse micron size gas bubbles -size control – new microfluidic tool to mass generate highly controlled monosized micro-bubbles. Similar configuration is used also for generation of liquid micro-droplets

Gas stream is surrounded by a much slower and denser coflowing liquid stream

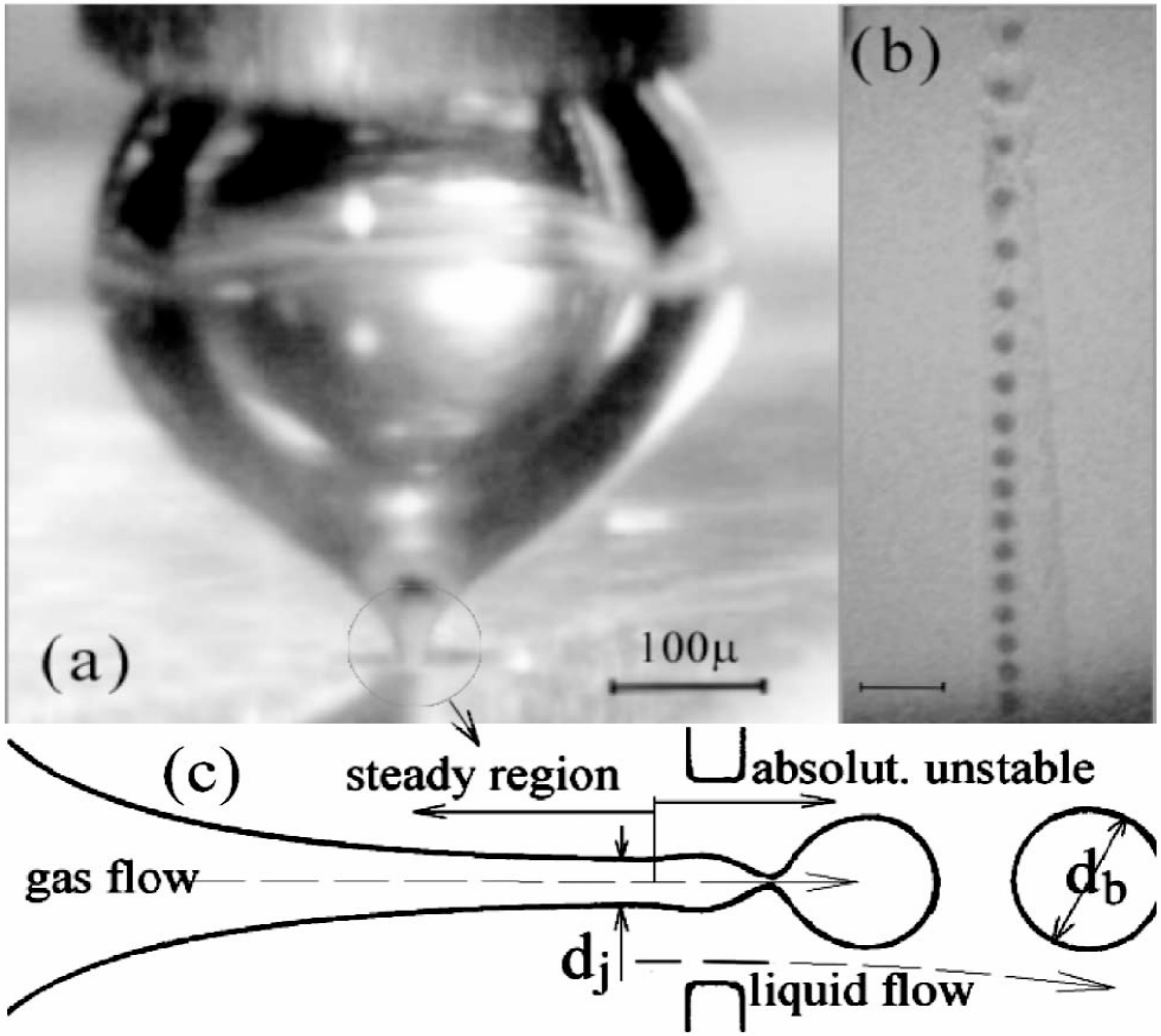

FIG. 1. (a) Cusplike bubble, attached to a capillary gas-feeding tube, from whose cusp a gas ligament issues through the orifice placed in front of the capillary. (b) Stream of gas bubbles issuing from the orifice. Picture taken with an exposure time of 1 μs. (c) Sketch of the region about the exit orifice, showing the steady and absolutely unstable regions of the gas ligament.

Physical mechanism of monodisperse gas bubble formation

The physical explanation of the radically different behavior of a laminar gas ligament from a laminar liquid ligament results on the absolutely unstable nature of the gas ligament, contrarily to the convectively unstable behavior of liquid ligament.

Thus, the absolute instability of the gas ligament provokes its rapid break-up into micro-bubbles. In addition, the nonlinear evolution of the local break-up of the ligament at the orifice involves a “self—excited” globally stable nonlinear saturation state (a limit cycle) with a saturated limit cycle amplitude.

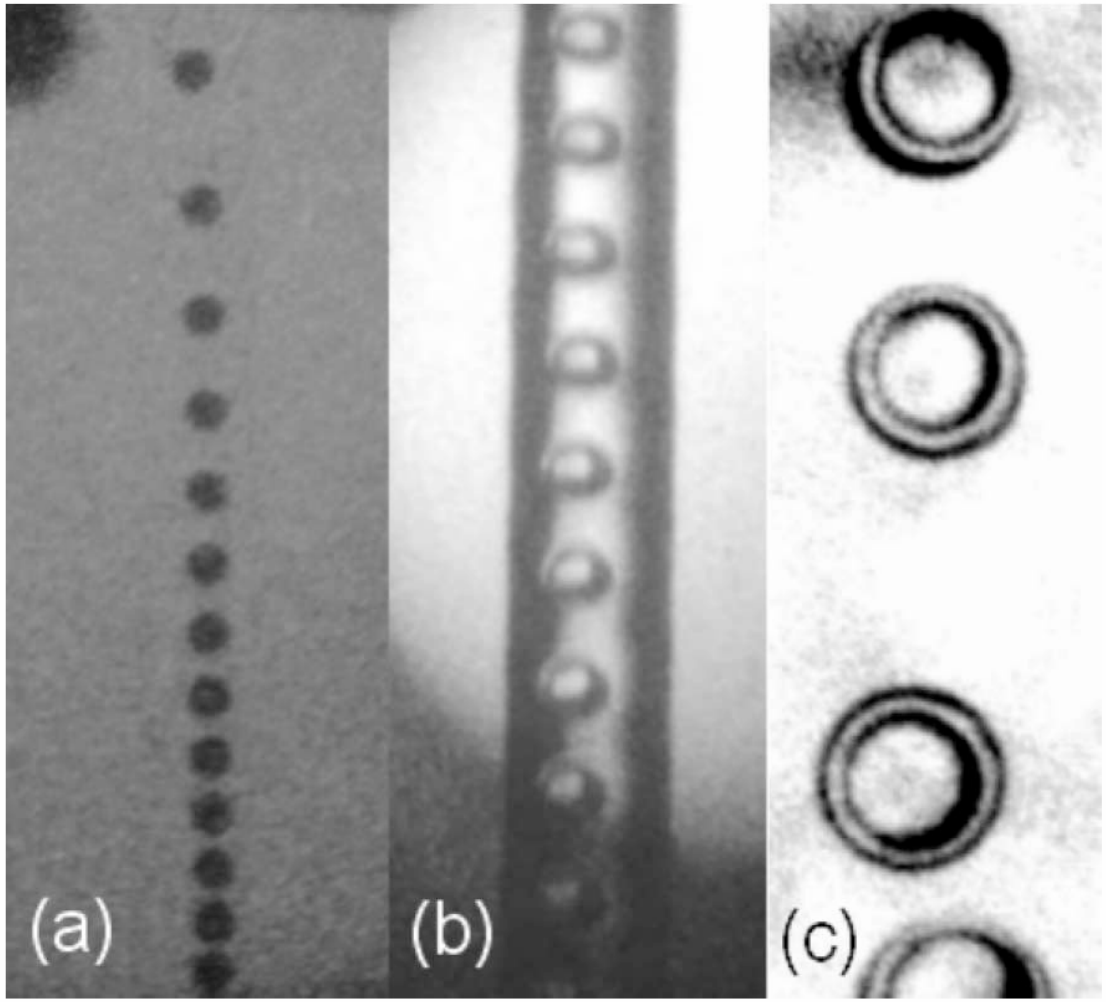

FIG. 2. (a) The liquid used to focus the gas is expelled into the same liquid. (b) The liquid with the gas bubbles is expelled into air, and a gas filled liquid jet with the diameter of the orifice is produced. This liquid jet eventually breaks up into equal-size gas filled microcapsules (c). Pictures taken with an exposure time of 11 μs. Arbitrary parameters (liquid: water +20% ethanol).

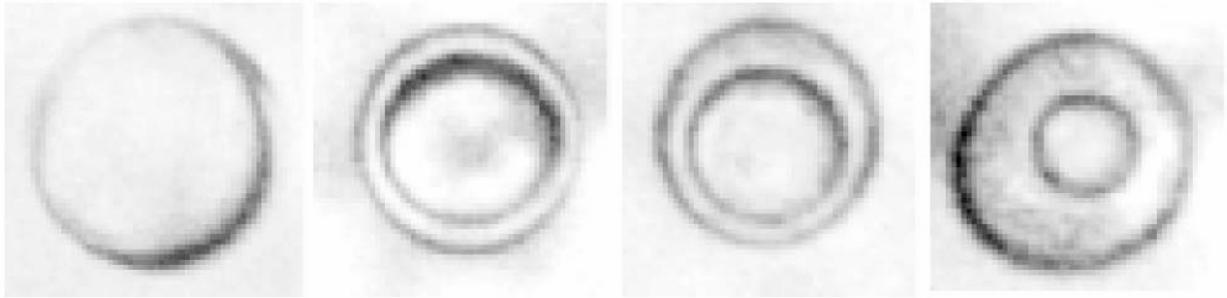

FIG. 3. Four examples of gas filled microcapsules that can be produced by this technique, by controlling the injected gas-liquid flow rates ratio $Q_g/Q_l = 8, 0.5, 0.1, 0.03$ (from left to right). Liquid: water +20% ethanol.

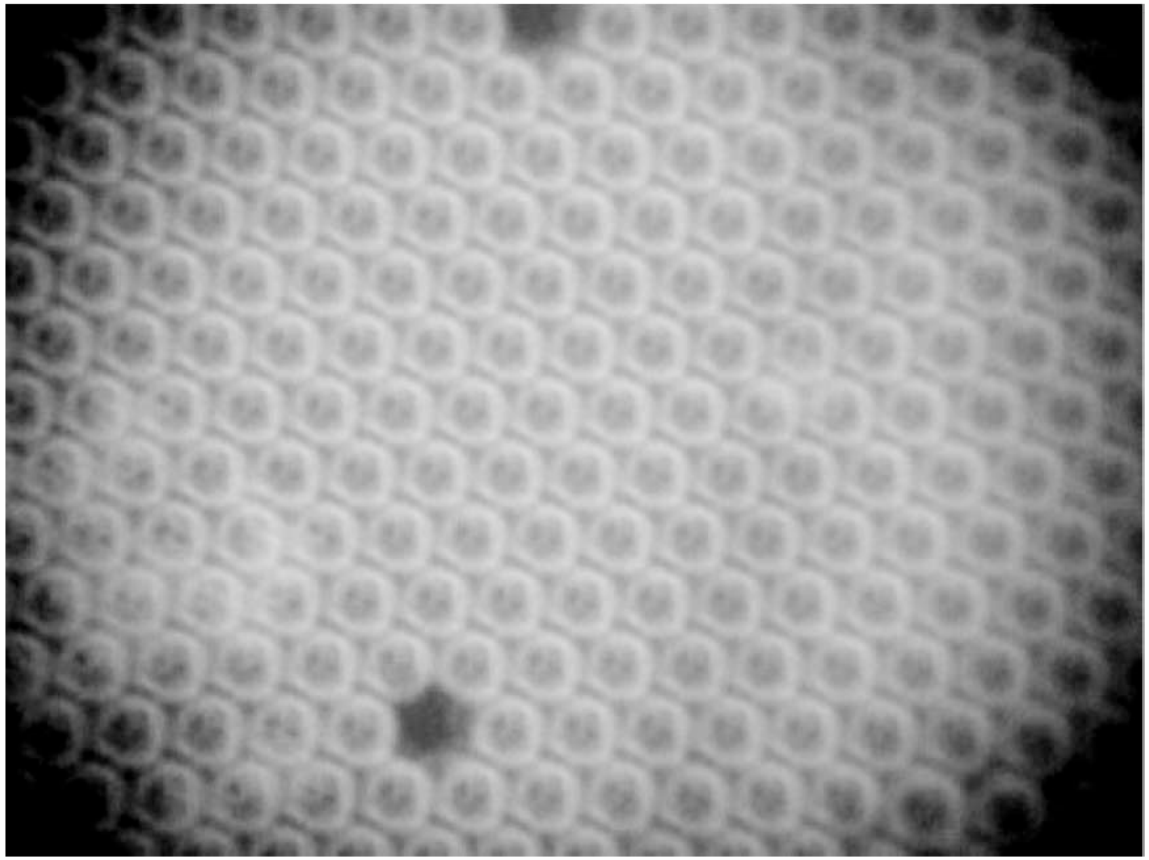

FIG. 4. When our microbubbles rise and settle, they form in many cases a "mesocrystal foam" or lattice. Bubbles are virtually *equal* in size, here 75 μm. Arbitrary parameters (liquid: water +45% glycerol).

Experimental analysis

The orifice diameter D from 500 down to 30 microns and viscosities from 0.001 to0.1 Pas were studied. Here a total 280 bubbles with d_b and D =100-210 μm

$$Q_l = 24-310\mu l/s; Q_g = 0.2-40\mu l/s;\ \mathrm{Re}_l = 40-1000;\ \mathrm{Re}_g = 0.07-14$$

$$T = 298\pm 0.5K; \rho_g = 1.2kg/m^3, \eta_g = 1.8\times 10^{-5} Pa\cdot s$$

Seven different liquids (water-ethanol and water-glycerol mixtures) with viscosity in the range $\eta_l = 1.2-30mPa\cdot s$, surface tension In the range $\sigma = 35-57mN/m$, and liquid density $\rho_l = 795-1200kg/m^3$ have been used and micro-bubbles of $d_b = 5-120\mu m$ have been measured.

Linear stability analysis of a gas ligament shows that the growth rate of perturbations $t_c^{-1} = Q_l/d_j D^2$ provides the relevant time of the process.

continuation

At $\mathrm{Re}_g > 1$ one gets non-dimensional frequency $\omega \propto t_c^{-1}; \Omega = \omega t_c$

to be dependent on boundary layer thickness, δ and $\Omega = \Omega(\mathrm{Re}_g)$

At $\mathrm{Re}_g < 1$ is independent of Re_g . So

$$d_b = \left[6Q_g / \pi\omega\right]^{1/3} = \left(\frac{Q_g}{Q_l}\right) D^{2/3} d_j^{1/3} f(\mathrm{Re}_g)$$

$$f(\mathrm{Re}_g) = \left(6/\pi\Omega\right)^{1/3}$$

Here $d_j << D$ is the orifice exit

$$d_j = \left(\frac{\rho_g}{\rho_l}\right)^{1/4} \left(\frac{Q_g}{Q_l}\right)^{1/2} D\left(1 - \frac{\pi^2 \sigma D^4}{4 d_j \rho_l Q_l^2}\right)^{-1/4} \left(\frac{\phi_g}{\phi_l}\right)$$

obtained from Bernoulli's and Laplace's laws. As the result one can find that all these expressions are rather incentive to fluid properties and consistent with

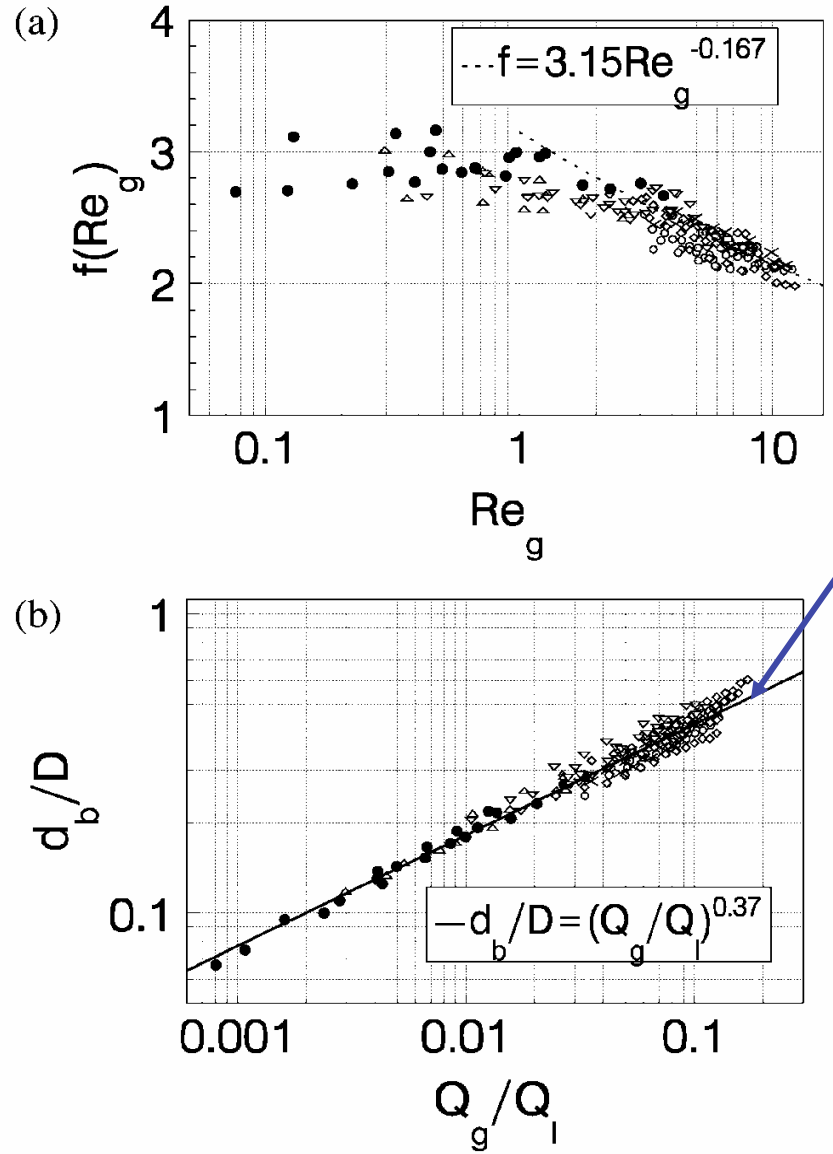

$$d_b / D \cong (Q_g / Q_l)^{0.37 \pm 0.005}$$

FIG. 5. (a) Experimental values of function $f(\mathrm{Re}_g)$. (b) Comparison of expression (4) with experimental values. Data points using $D = 210$ μm: ($\circ$) $\mu_l = 1.23$; ($\diamond$) $\mu_l = 1.87$; ($\square$) $\mu_l = 2.35$; ($\triangle$) $\mu_l = 10$; ($\bullet$) $\mu_l = 30$. Data points using $D = 100$ μm: ($\triangledown$) $\mu_l = 5$; ($\times$) $\mu_l = 10$. Viscosity unit: cpoise (10^{-3} Pa $\cdot$ s).

Ordered and disordered patterns in two-phase flows in micro-channels

R. Dreyfus,P.Tabeling,H.Williame, PRL **90**, 144501 (2003)

It is demonstrated that wetting properties of the fluid with respect to the walls are exceedingly important parameters in micro-size systems, so that below some size the system with untreated walls stops to produce well controlled structures

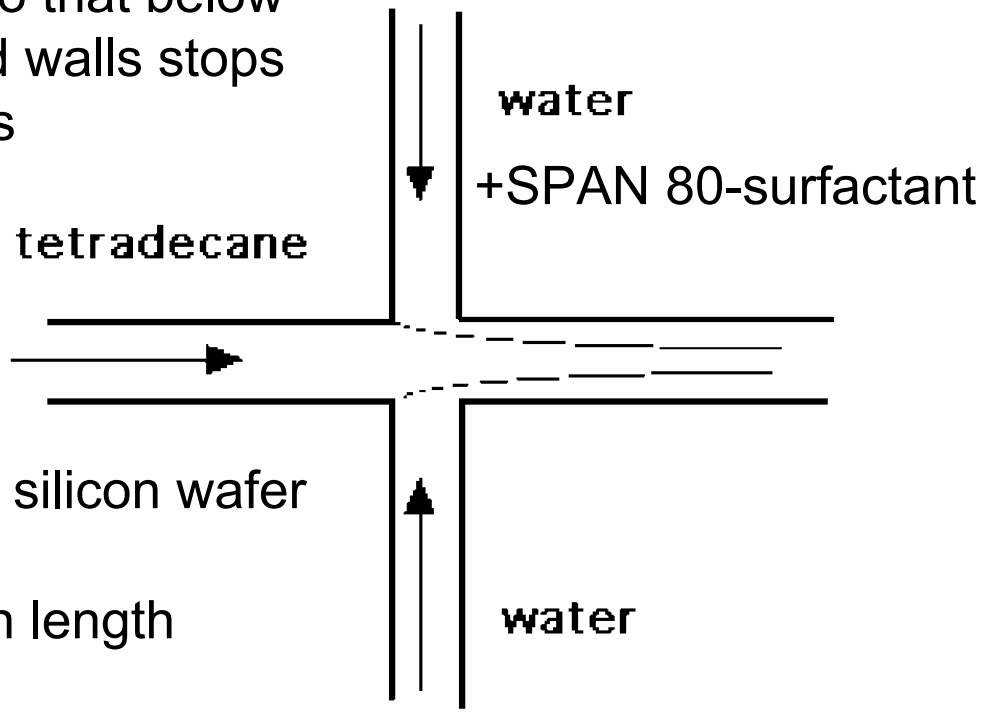

Micro-channel in glass covered by a silicon wafer

$20\mu m \times 200\mu m$ and 20 mm in length

FIG. 1. Scheme of one particular experimental configuration discussed in the Letter.

Contact angle of water drop immersed in tetradecane in contact with silicon and glass surface for different surfactant concentration (static experiment)

Partial water wetting Complete water dewetting

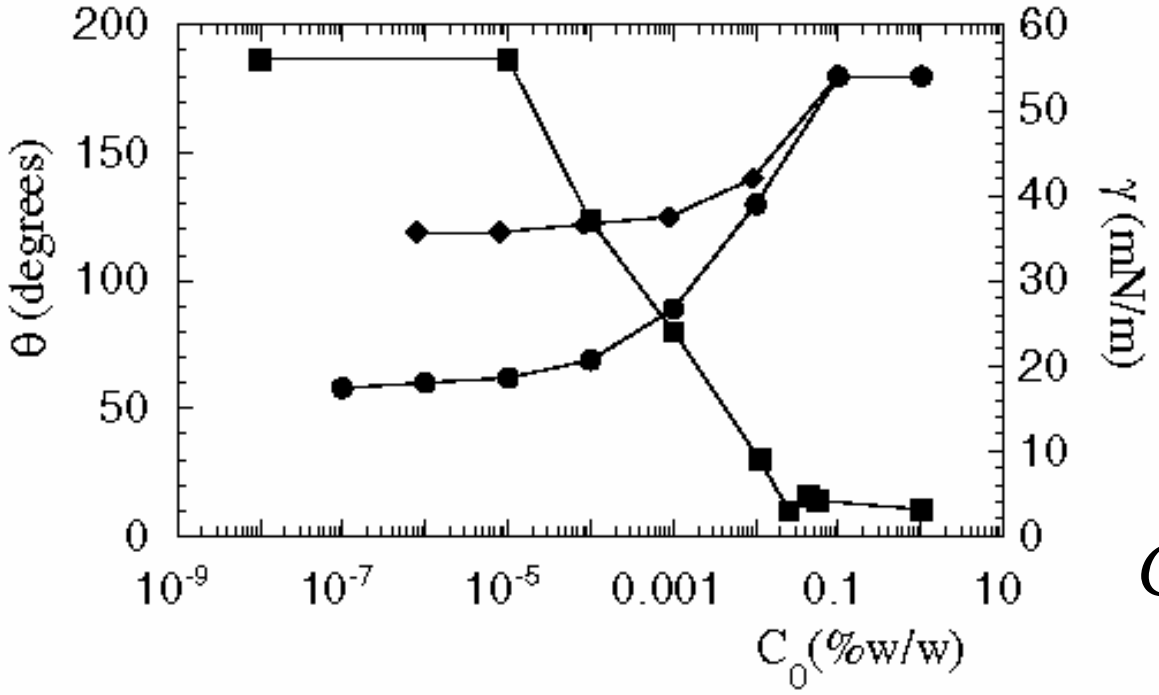

FIG. 2. Evolution of the contact angle with the surfactant concentration. Squares: interfacial tension; triangles: contact angle for silicon; circular dots: contact angle for glass.

Complete oil wetting is reached at the critical micellar concentration

$$C_{mc} \cong 3\times10^{-2}\%w/w$$

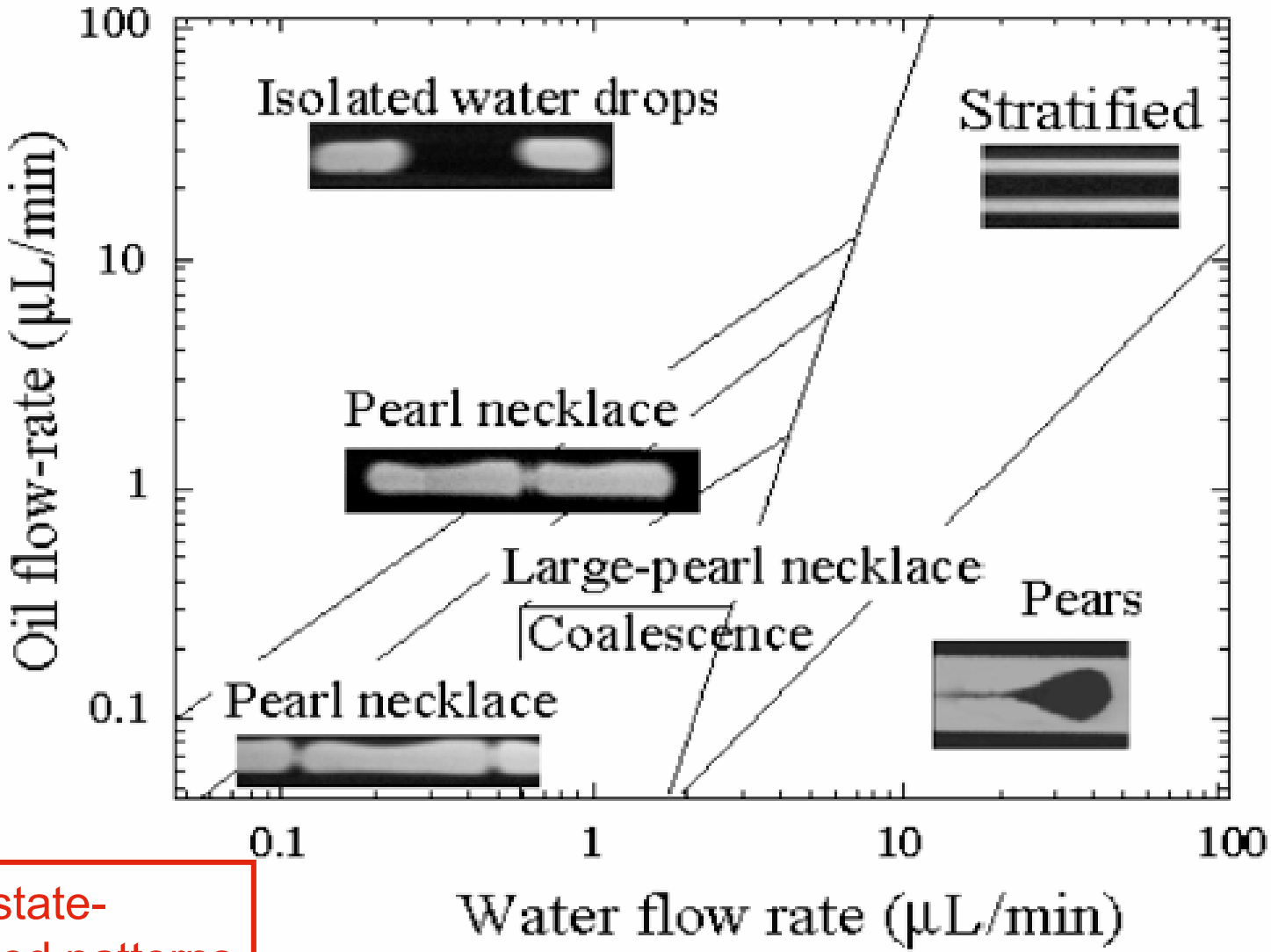

Dynamic state-
Well defined patterns

FIG. 3. Flow patterns in the complete wetting case. The diagram is established for a concentration $C_0 = 2.2\%$ w/w. About one hundred regimes have been analyzed to determine such a diagram. (depends on the entry conditions)

Dynamic process leading to drop formation (interfacial instability at lower water flow rate)

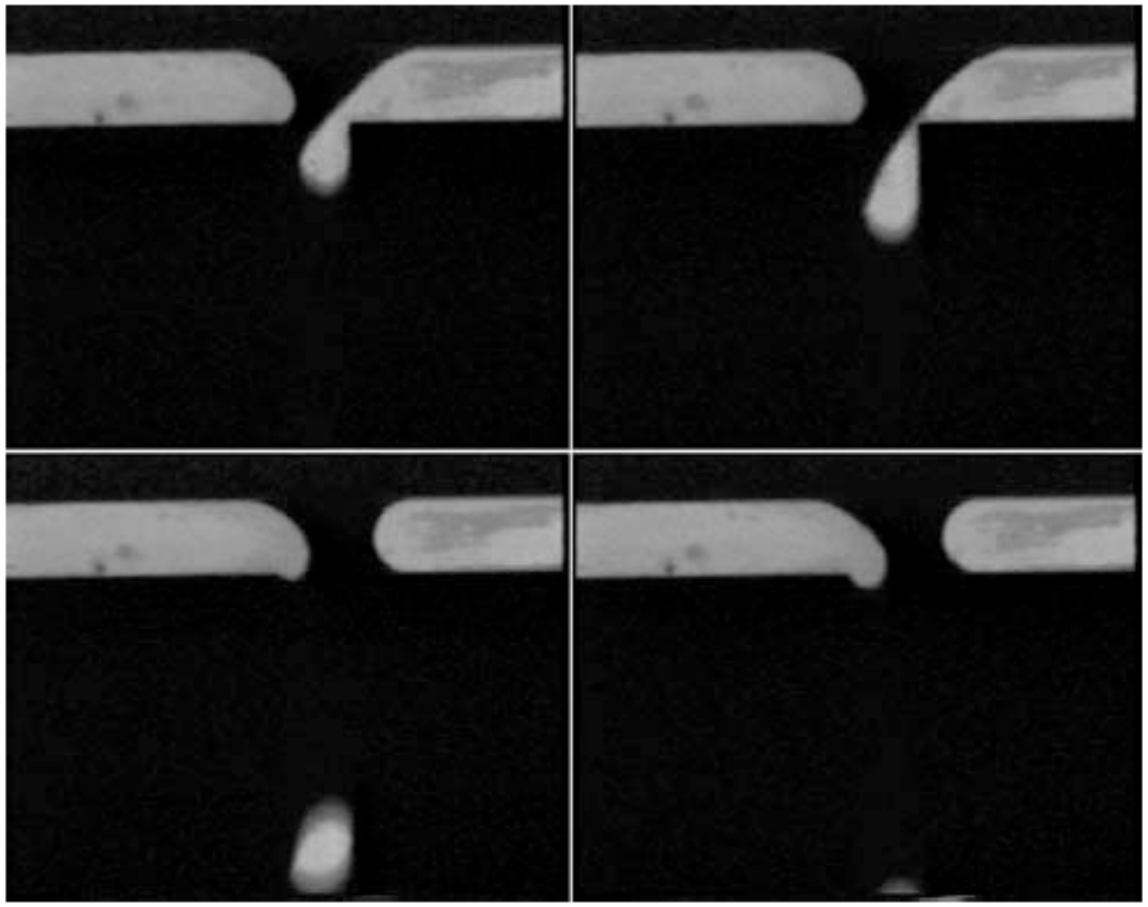

FIG. 4. Sequence of events leading to water drop formation. The drops are formed at the intersection of the channels. The channel cross-sectional dimensions are 20 μm $\times$ 200 μm; the time sequence between the first two pictures is 0.6 s.

Partial wetting case (low surfactant concentration)

Capillary forces dominate the system

$$Ca \equiv \frac{\eta V}{\sigma} \approx 10^{-3}$$

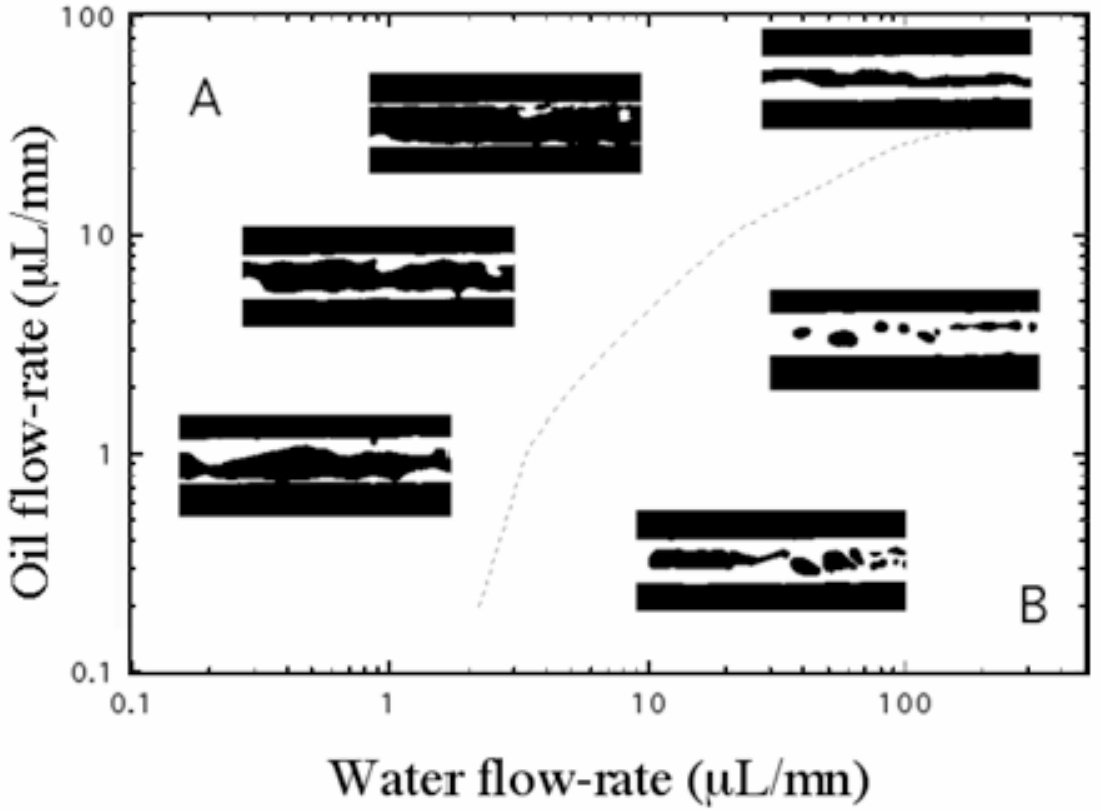

FIG. 5. Flow patterns obtained in the same conditions as in Fig. 3, but without surfactant.

System evolves continuously from structureless to structured configuration by varying surfactant concentration in T configuration

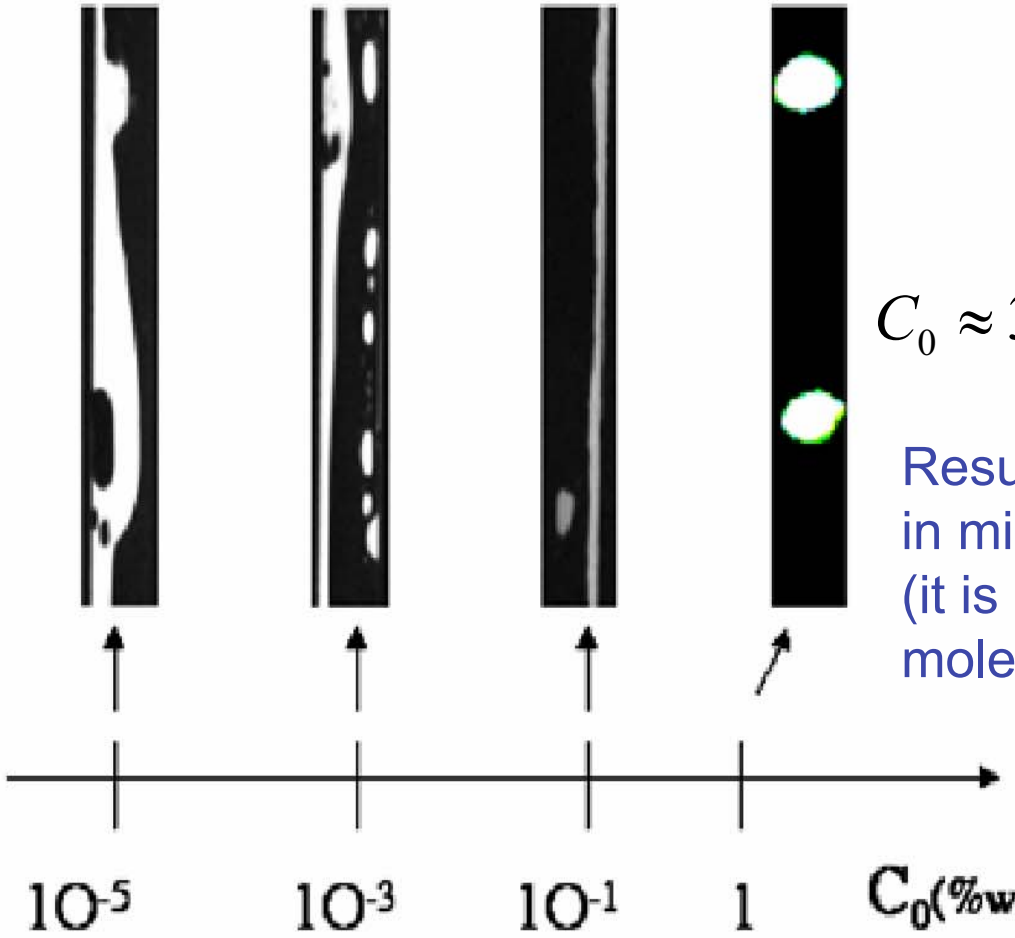

Transition at

$$C_0 \approx 3\times10^{-1}\%w/w >> C_{mc}$$

Result of small droplet size in micro-channels (it is sufficient surfactant molecules at C_{mc})

FIG. 6 (color online). Evolution of the flow patterns with the SPAN 80 concentration, using a T configuration. Oil is injected from the right; the flow rates for the two liquids are 0.1 μl/mn.

Lower limit for the channel depth, ***b***, for controlled structures

$$C_0 v = 2C_{surf} S + C_v bS$$

(*v*=*Sb*-drop volume)

$$C_v = C_{mc}$$

$$C_{surf} = C_{sat}$$

$$b = \frac{2C_{sat}}{C_s - C_{mc}}$$

$$\boxed{b_{\min} \approx 60nm}$$

$C_s = 0.2 mol/dm^3$ -is the solubility limit

$C_{sat} = 5.5 \times 10^{-8} mol/dm^2$ -is the saturation value

Drop formation in a flow-focusing configuration in a micro-device

S.Anna, N.Bountoux, H.Stone, Appl.Phys.Lett. **82**, 364 (2003)

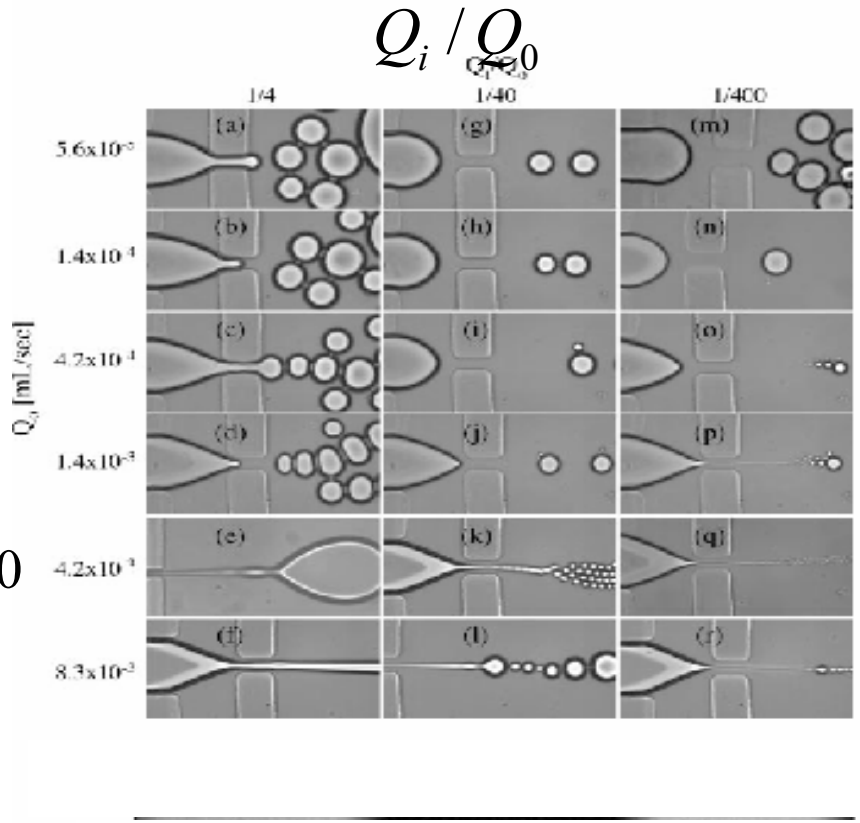

0.67% SPAN-80 added to oil

Q_i -water flow rate

Q_0

Stability diagram for drop formation
in flow-focusing micro-configuration

Geometrically mediated breakup of drops in microfluidic devices

D.Link et al, PRL **92**, 054503 (2004)

How does one break larger droplets into smaller ones in controlled way?
T-junction and flow past isolated obstacle and emulsion of water and oil flow (surfactant used to stabilize the droplets)

Conventional emulsification techniques use inhomogeneous extensional and shear flows to rupture droplets and to generate emulsions with wide distribution in droplet sizes. How to reduce polydispersity?

1. By shearing between plates
2. By single-drop technologies

T-junction $r_0 \approx d$ breaking of drops in extensional flow

Water drops in continuous phase of hexadecane + SPAN-80 3%wt

$$\sigma = 5mN/m; \eta = 8\times10^{-3}\, Pa\cdot s$$

Polydispersity less than 1-3%

There is a critical flow rate above which the drops always break

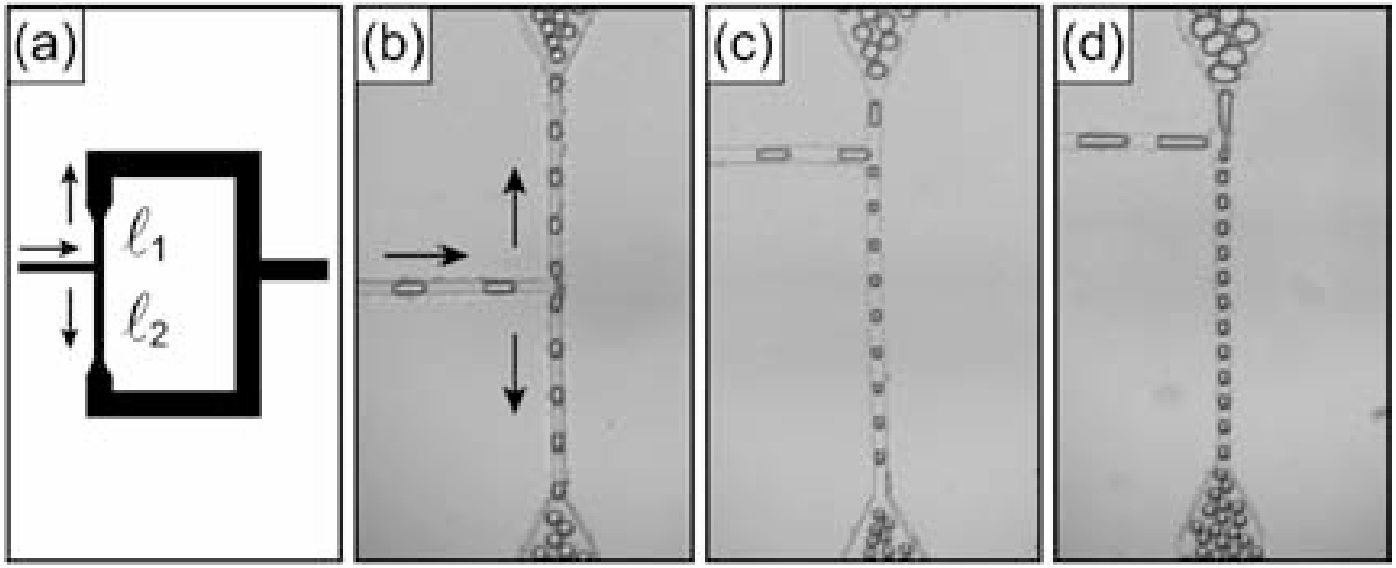

FIG. 1. Passive breakup at T junctions. Droplets flow into a T junction, sketched in (a), where the flow is split into two sidearms. The narrow portion of the two side arms, of lengths ℓ_1 and ℓ_2, control the relative flow resistance of the paths and, hence, the relative sizes of the two daughter drops as shown in the photomicrographs of (b), (c), and (d); the ratios of arm lengths are, respectively, $\ell_1/\ell_2 = 1{:}1$, 1:5.2, and 1:8.1, corresponding to daughter drop volume ratios of (b) 1:1, (c) 1:5.2, and (d) 1:7.5.

Asymmetric breakup of droplets-
analog of an electric-current-splitting device

$$\Delta p = \beta g l$$

$$\beta \approx \eta(3/4)\left[1/(w_0 h^3)\right] \times \left[1 - 6(2/\pi)^5 (h/w_0)\right]^{-1}$$

$$q_1 / q_2 \approx l_2 / l_1 \propto V_1 / V_2$$

$$C_G = \eta G a / \sigma$$

Extensional flow capillary number,
a- undeformed drop radius

$$G \approx v / w_0; C_G = Ca / w_0$$

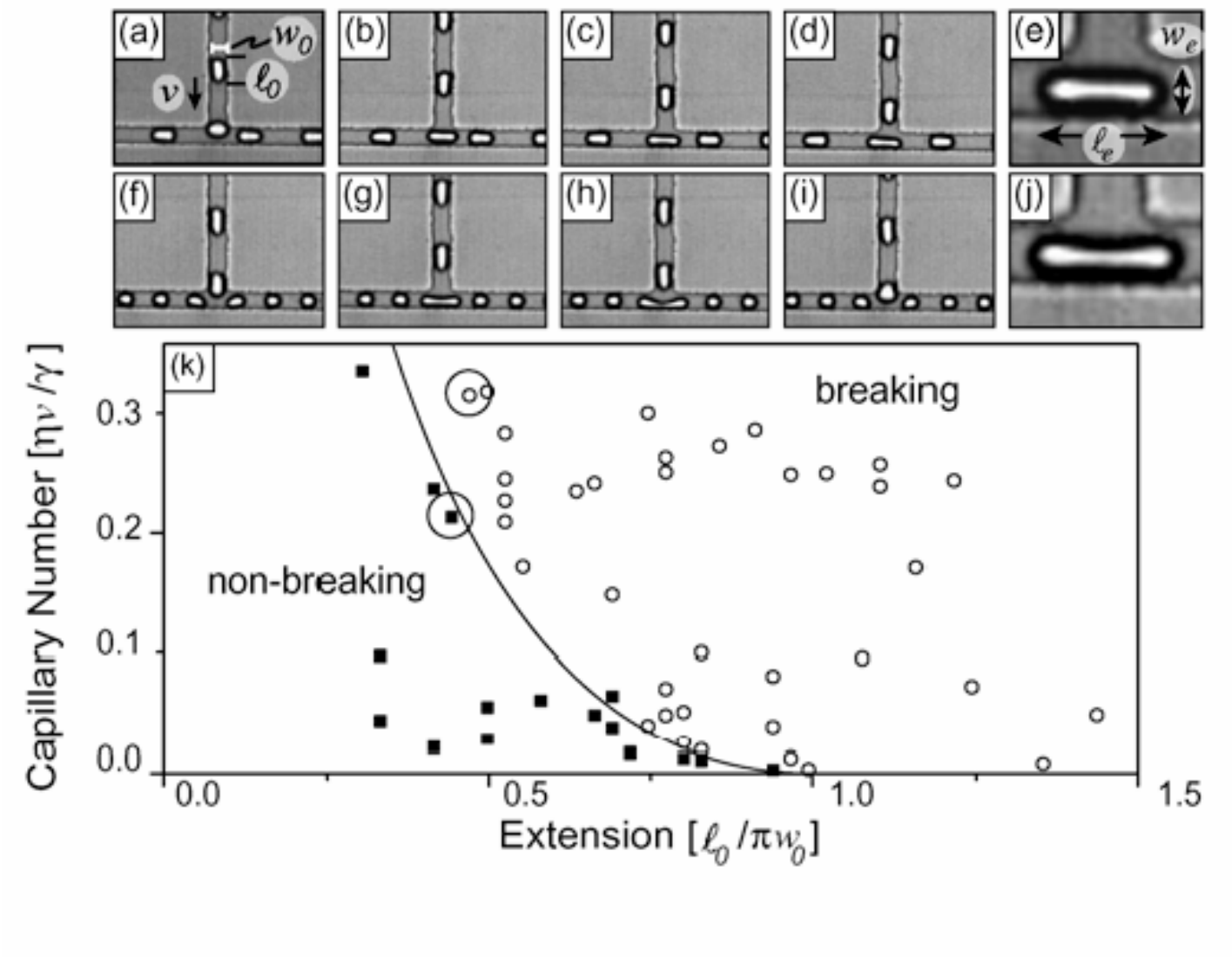

Critical condition for breakup droplets

$$l_{ext} - l_0 \propto (G - G_0)^{1/2}$$

$$G_0 << G \Rightarrow C_G \propto (l_{ext} / a - l_0 / a)^2$$

$$l_{ext} / \pi w_e = 1; \varepsilon_0 = l_0 / (\pi w_0); \varepsilon_e = l_e / (\pi w_e)$$

$$l_0 w_0^2 = l_e w_e^2 \Rightarrow C_{cr} = \alpha \varepsilon_0 (1 / \varepsilon_0^{2/3} - 1)^2$$

FIG. 2. Critical conditions for breaking drops at T junctions. In a channel of width w_0, droplets having length ℓ_0 and velocity v enter a T junction and either break or do not break. An example of nonbreaking drops, corresponding to the circled point below the curve in (k), enter the T junction in (a), stretch in (b), reach a maximum extension in (c), and then move alternatively left and right out of the junction in (d). At maximum extension, shown in (e), the extended length ℓ_e and width w_e give $\varepsilon = \ell_e/(\pi w_e) = 0.95$. A similar series for breaking conditions corresponding to the circled point above the critical line are shown in (f)–(i). In this case, the maximum extension shown in (j) is $\varepsilon = 1.15$. In (k), open circles indicate when drops of a given capillary number $C = \eta v/\gamma$ and initial extension $\varepsilon_0 = \ell_0/(\pi w_0)$ break, and squares indicate when they do not. A model for the critical capillary number for breaking C_{cr} provides the curve $C_{cr} = \alpha\varepsilon_0(1/\varepsilon_0^{2/3} - 1)^2$ shown in (k) with fitting parameter $\alpha = 1$.

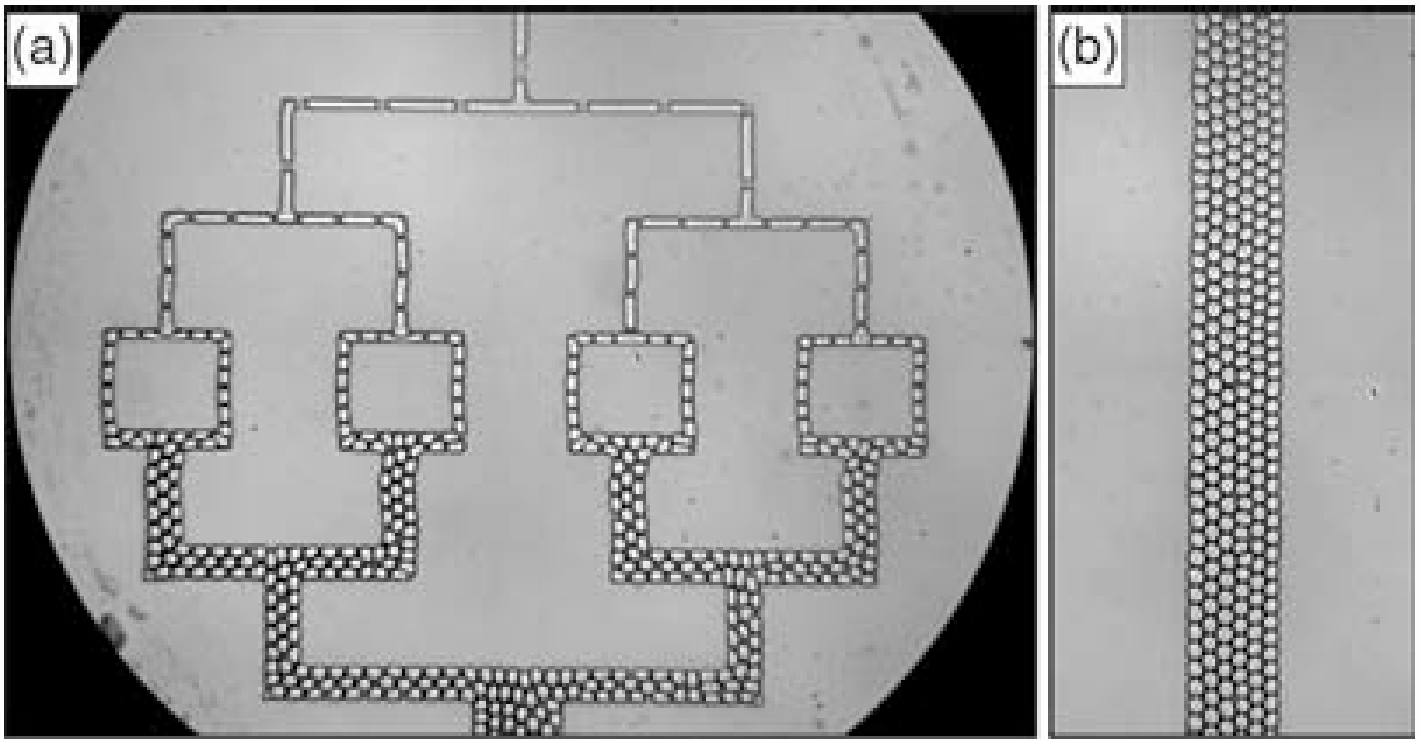

FIG. 3. Sequential application of passive breakup. In (a) drops are formed at high dispersed phase volume fractions (drop formation not shown) and are sequentially broken to form small drops. In (b) the droplets flow downstream with nearly defect-free hexagonal-close-packed ordering.

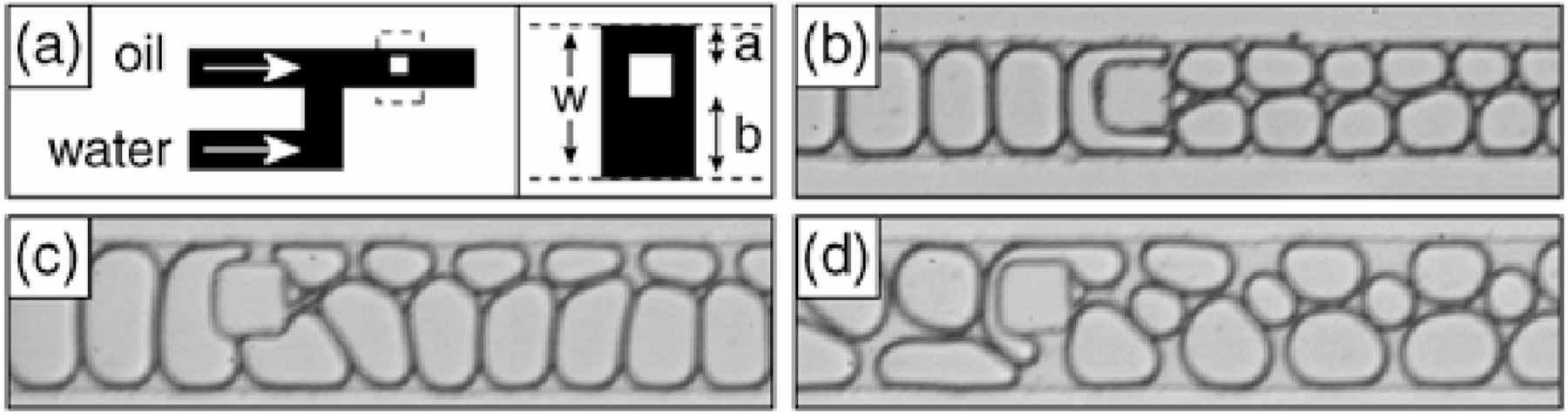

FIG. 4. Obstruction mediated passive breakup. (a) Schematic diagram of a square obstruction in a microchannel. The obstacle is a 60 μm square; $a = 15$ μm. (b) The obstacle is approximately in the center of the channel so that the ratio a/b is 1:1.2. (c) The channel width is 120 μm and the ratio a/b is 1:2.7. (d) As in (c) but every second drop breaks when a two-layer pattern encounters an off-center obstruction.

Microfluidic network for rapid mixing without dispersion

New microfluidic technology that relies on piko-L droplets to mix the reagents rapidly (less than 1 ms) and to transport them with no dispersion.
These microfluidic networks use fluid flow to convert spatial evolution of chemical systems into temporal evolution (convert distance into time).

Using this technology to understand the dynamics of complex chemical systems

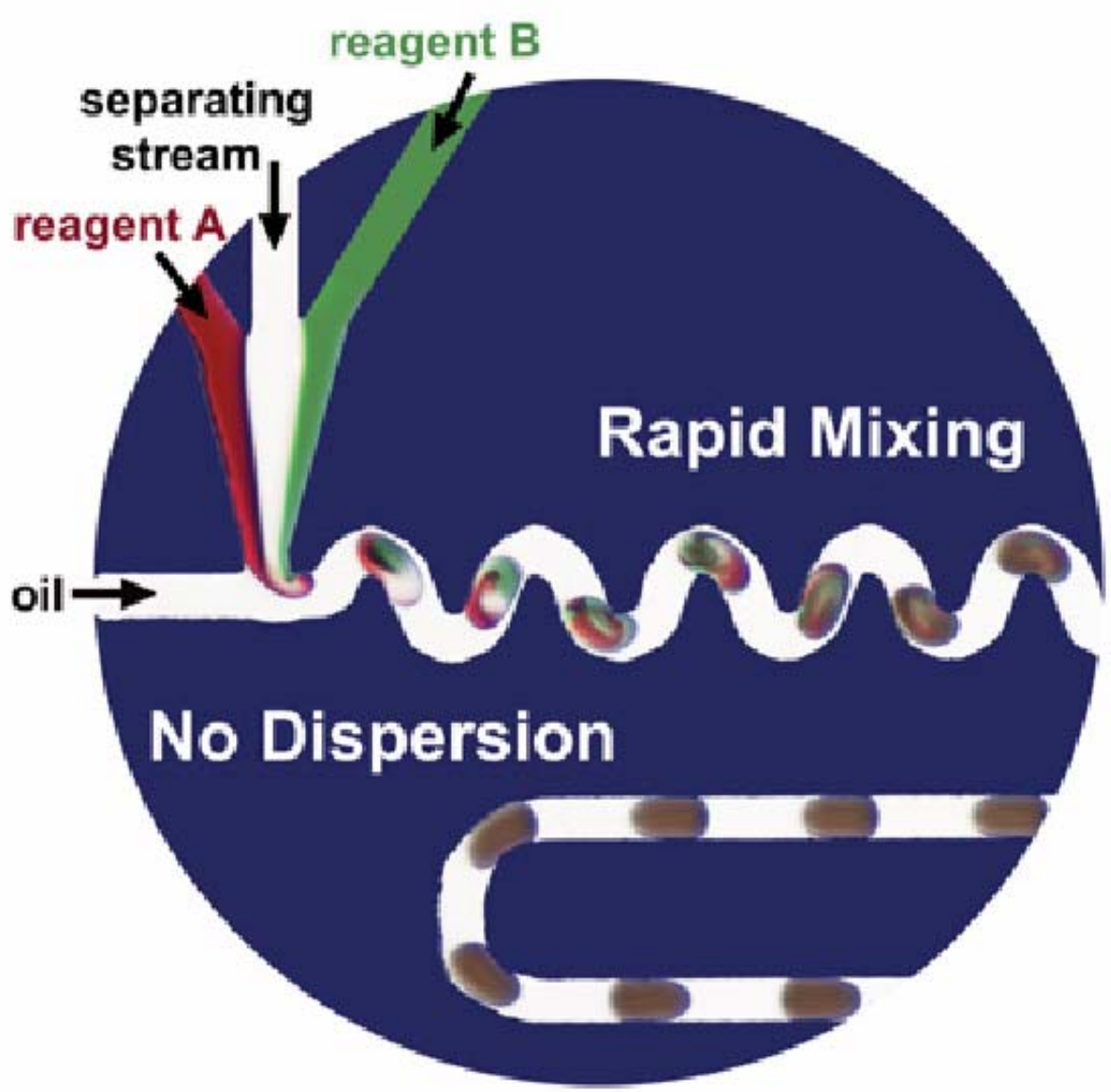
reagent B
separating
stream
reagent A
Rapid Mixing
oil
No Dispersion

Chaotic mixing in droplets

R. Ismagilov et al

The concept of induced chaotic mixing in unsteady, time-periodic flows inside droplets moving through winding micro-channels (Song et al 2003) was used especially to perform kinetic measurements on msec time scale (Song & Ismagilov(2003))

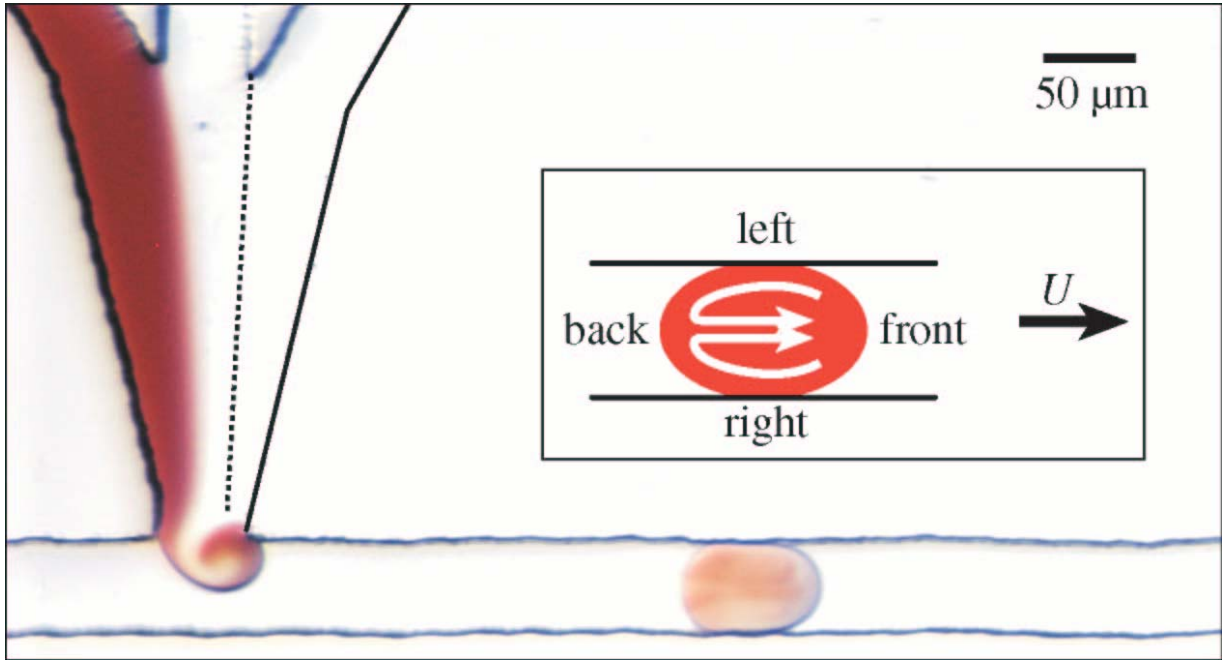

Non-chaotic mixing
in droplets

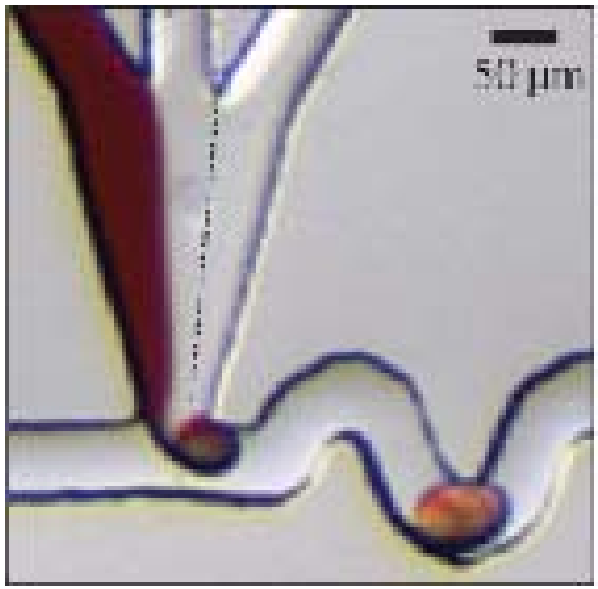

Chaotic mixing
In droplets

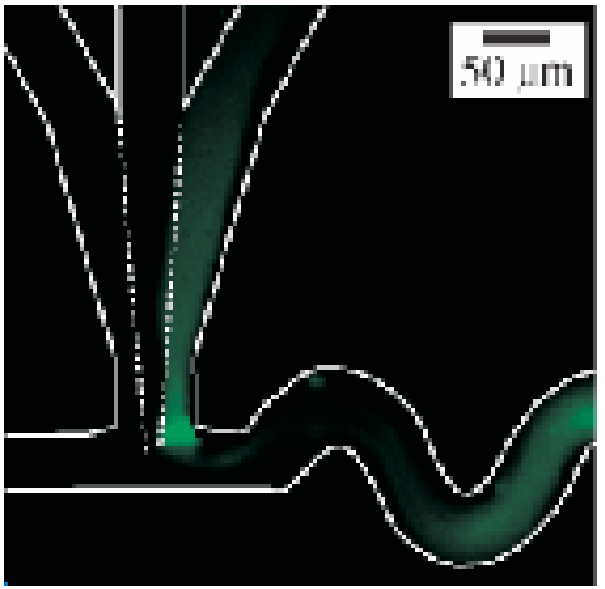

R.Ismagilov et al

Chaotic mixing in droplets

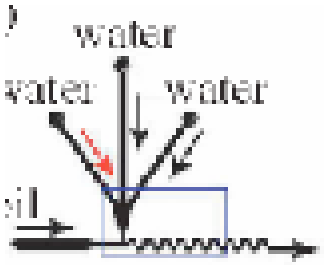

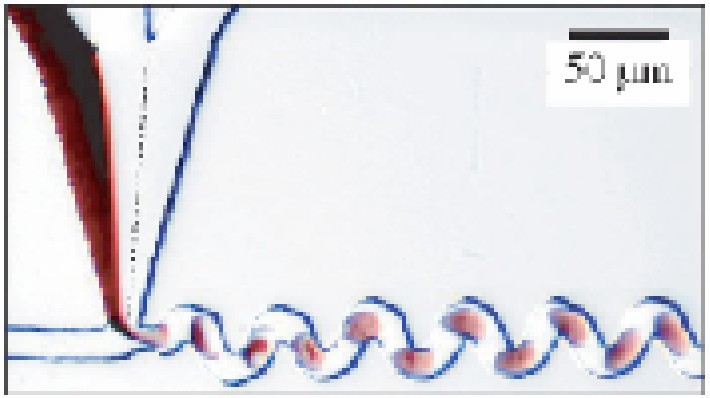

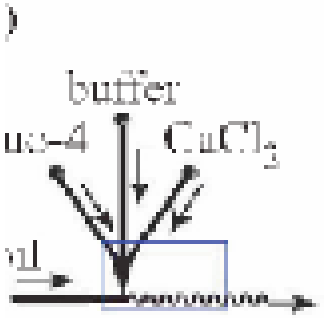

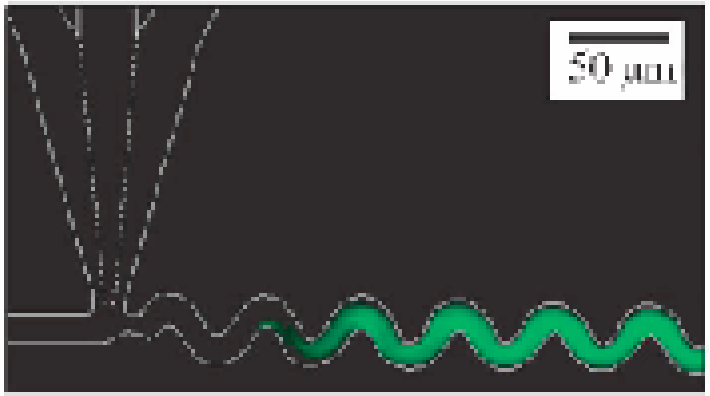

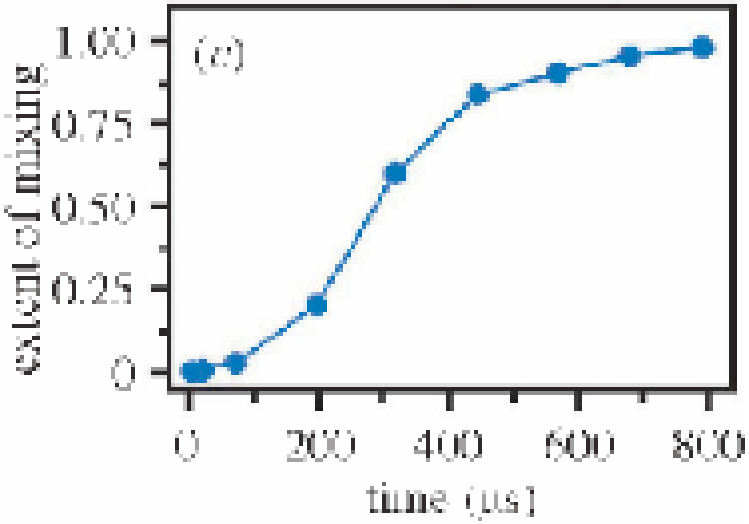

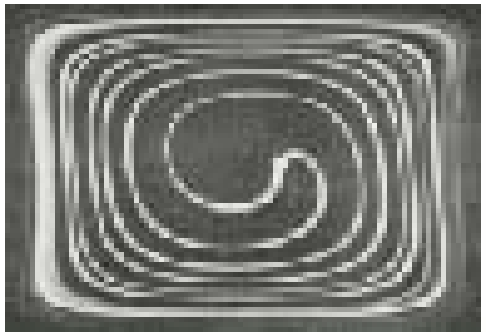

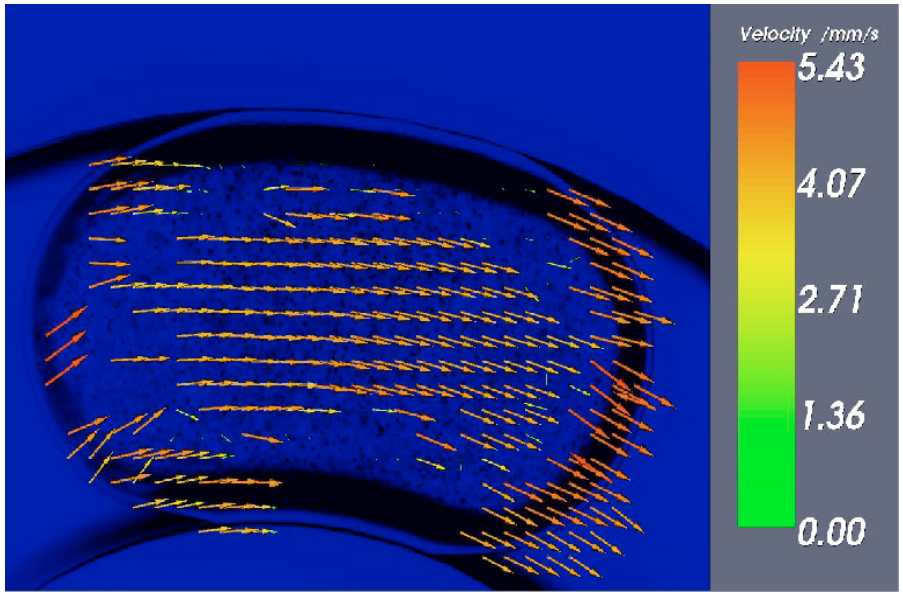

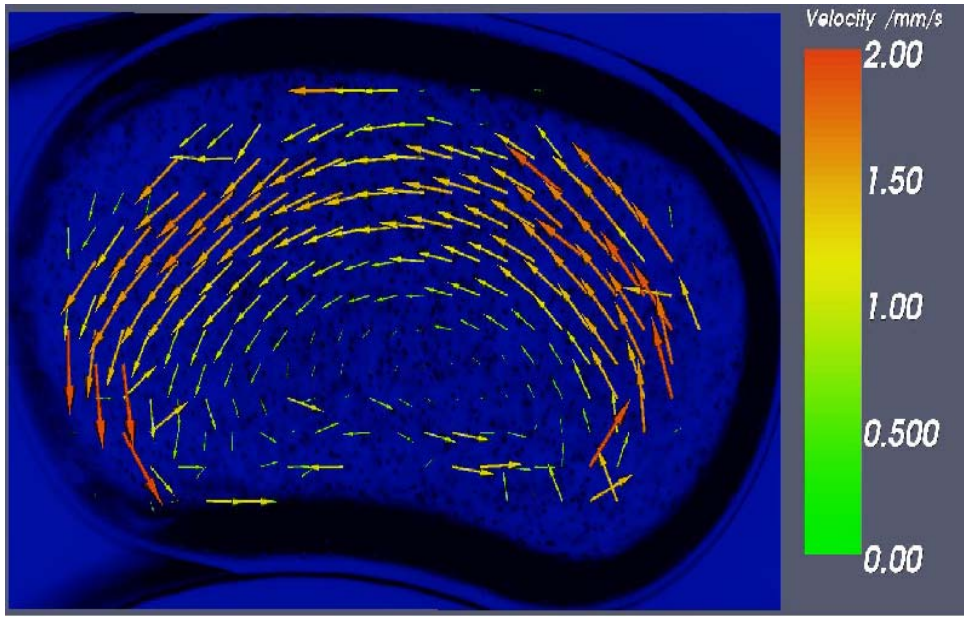

global flow
4mm/s

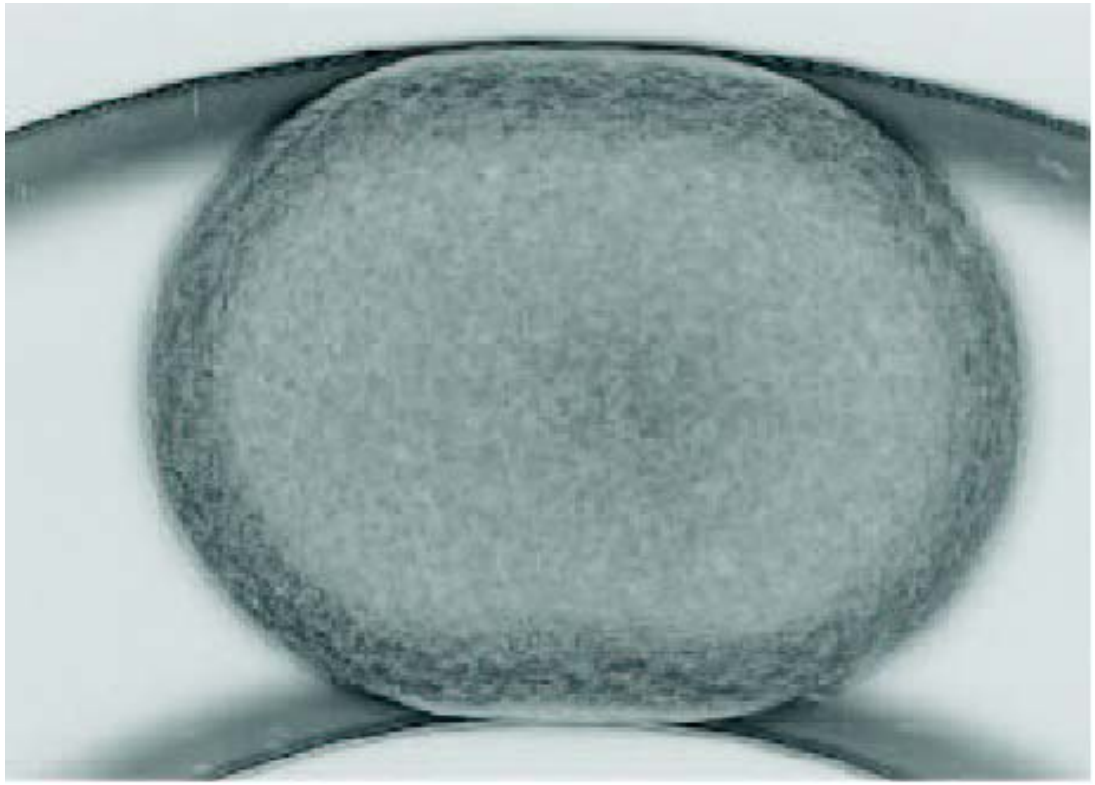

Internal flow

T. Henkel et al Delft
(2005)

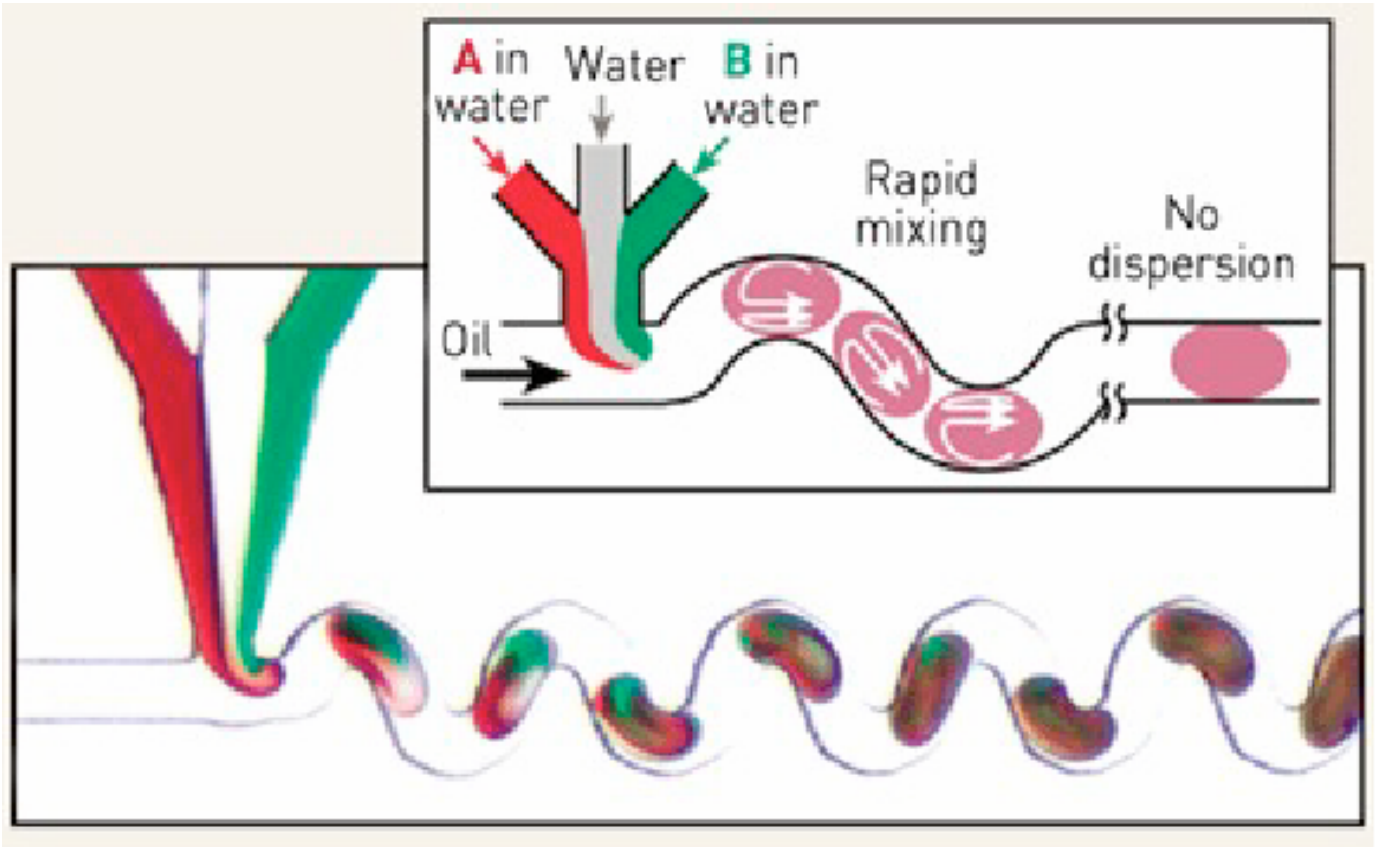
A in water
Water
B in water
Rapid mixing
No dispersion
Oil

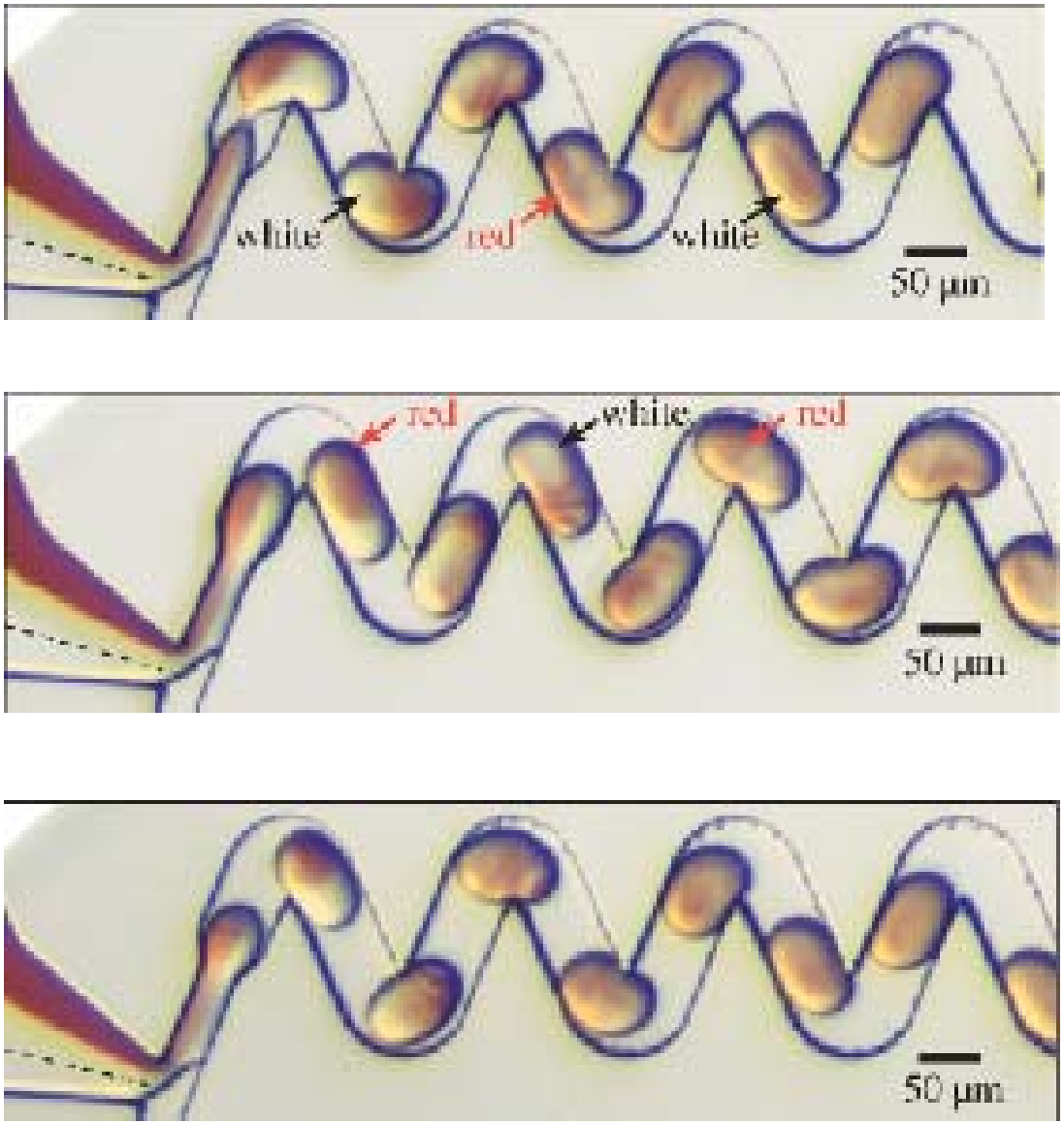
white
red
white
50 µm
red
white
red
50 µm
50 µm

Conclusion

- Phase internal flow is controlled by interface friction at liquid/wall and liquid/liquid interfaces.
- Dependence on phase ratio and flow velocity superposition of both effects is found.
- Both – wall friction as well as interface friction dominated flow have been analyzed.
- Asymmetric flow fields for enhanced mixing can be generated in winding channels.
- In curved micro-channels both - wall friction and interface friction dominated flow - result in enhanced mixing efficiency, but different flow field characteristics.

Vesicle orientation and dynamics in shear flow

V.Kantsler and V. Steinberg, submitted to PRL (2005)

WEIZMANN
INSTITUTE
OF SCIENCE

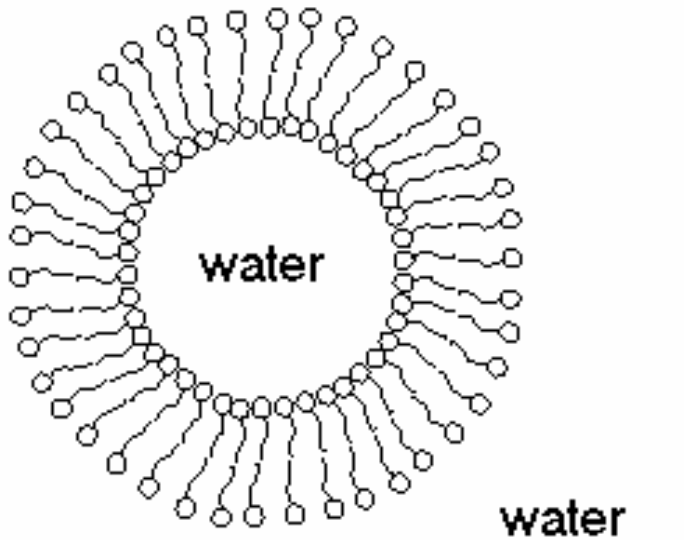

Vesicle is a spherical phospholipid membrane with a thin wall, that is about some tens of nanometers

DMPC-phospholipid molecule

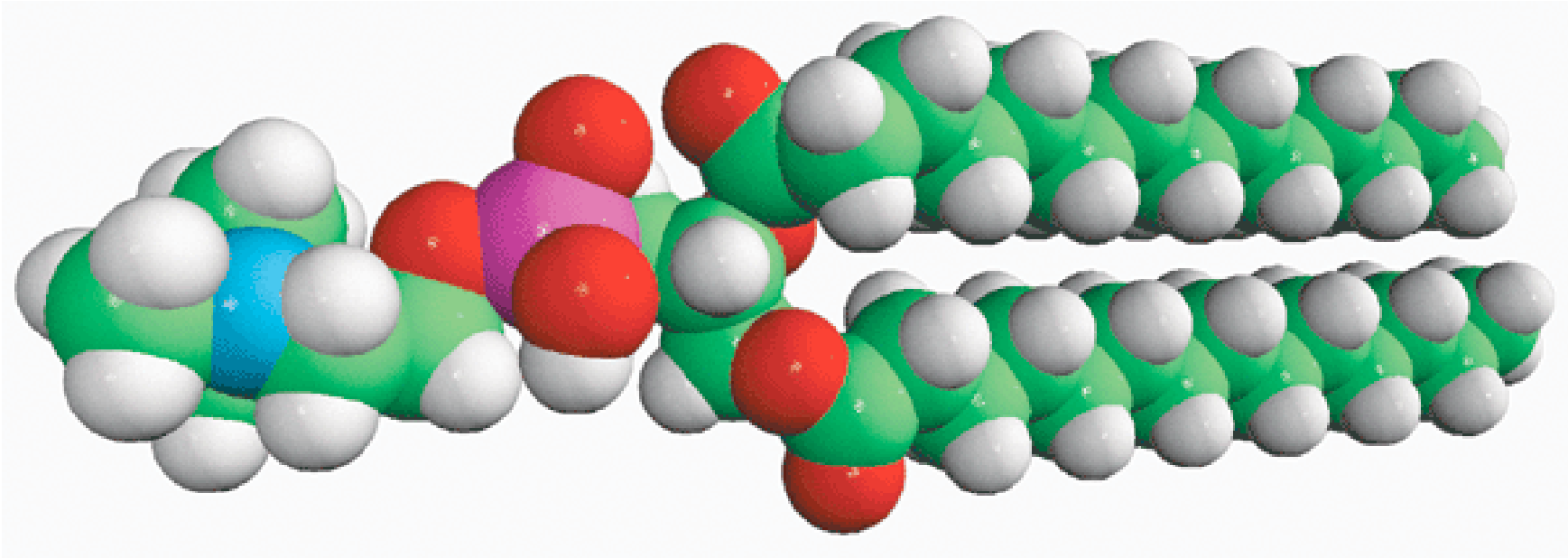

Polar «head»

Hydrocarbon «tail»

Giant unilamellar vesicles are used to simulate blood cells behavior, since this simplified model can be well described analytically.

When an object is placed to a shear flow it is forced by torque associated with rotational component of shear and a stretching and torque due to elongation component. The resulting vesicle dynamics depend on the competition of these two components of the flow.

Dynamics of deformable mesoscopic objects under hydrodynamic stresses determine rheology of many complex fluids, such as suspensions of droplets or bubbles, emulsions, solutions of vesicles, blood, biological fluids, etc

Equation of motion of a vesicle has a form

$$\dot{\phi} = A\sin^2\phi - B + F, \qquad \phi \text{ - inclination angle;}$$

A, B - coefficients characterizing the competition;

F - noise term

In the absence of *noise*, the stationary solution exists at |A/B|<1.
It is also known that vesicles similar to blood cells can exhibit so called tank treading motion (it undergoes thermal fluctuation around the mean value only) and the membrane rotates around its interior.

The experiment is aimed to describe this type of motion, inclination angle And its fluctuations of a single vesicle as a function of its excess area, shear rate, viscosity and viscosity contrast.

$\Delta = S / R^2 - 4\pi$; excess area

$\varepsilon = \eta_{in} / \eta_{out}$; viscosity contrast

$\chi = \dot{\gamma}\eta_{out} R^3 / \kappa$; dimensionless shear rate

$V = \frac{4}{3}\pi R^3$ effective vesicle radius defined via volume

Experimental set-up

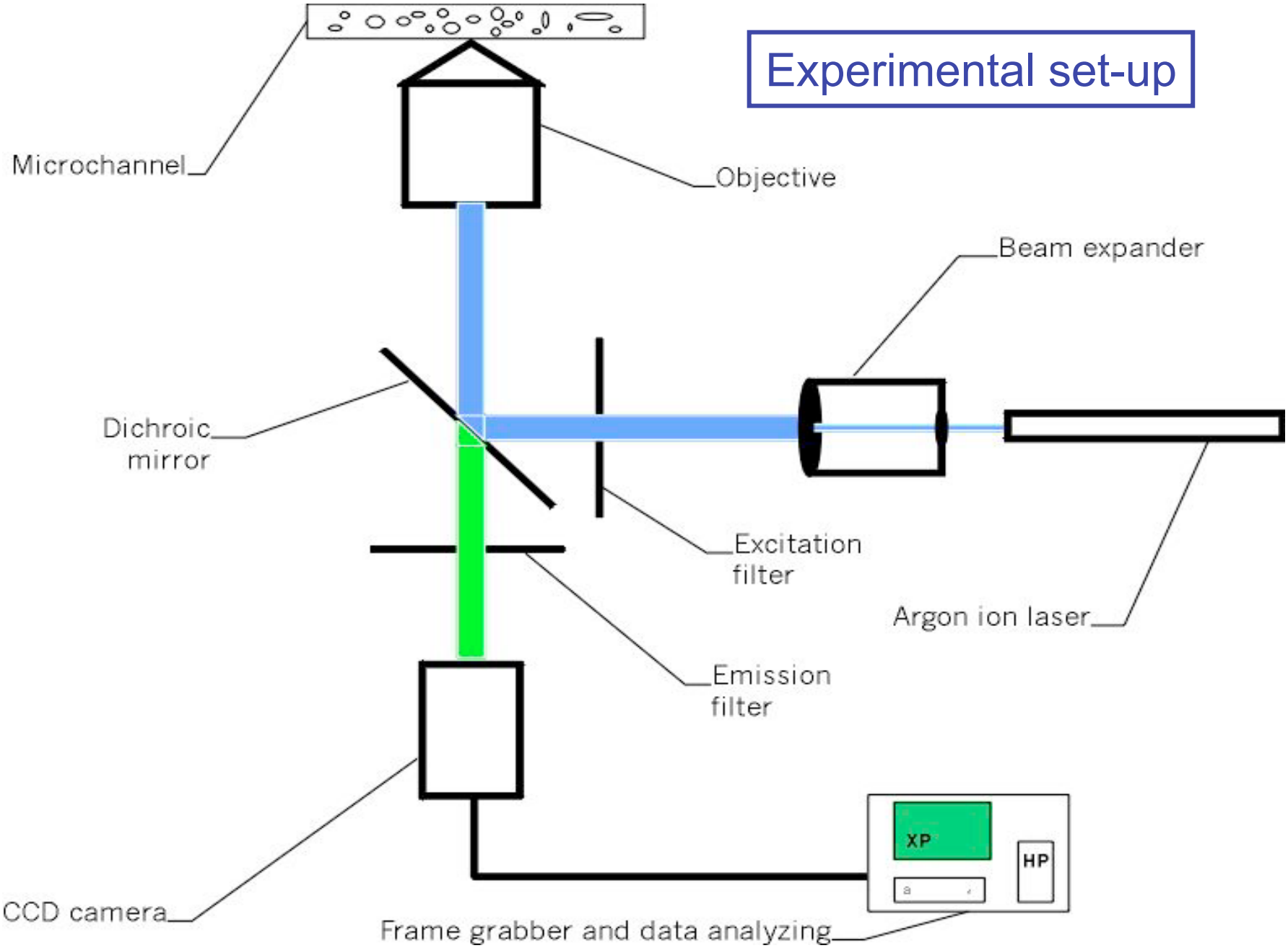

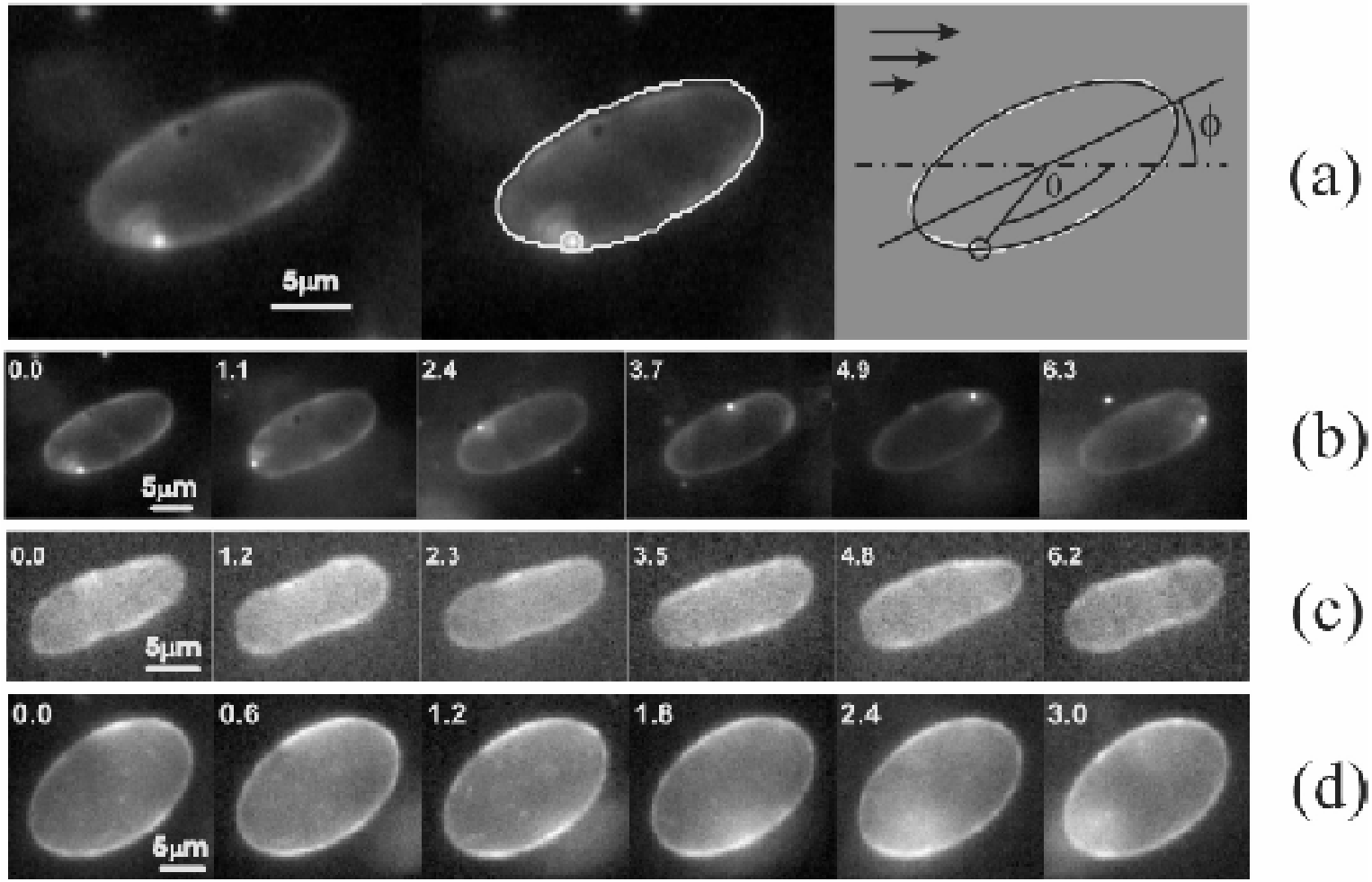

Snap shots of vesicles at low (c) and high (d) viscosities and various excess areas

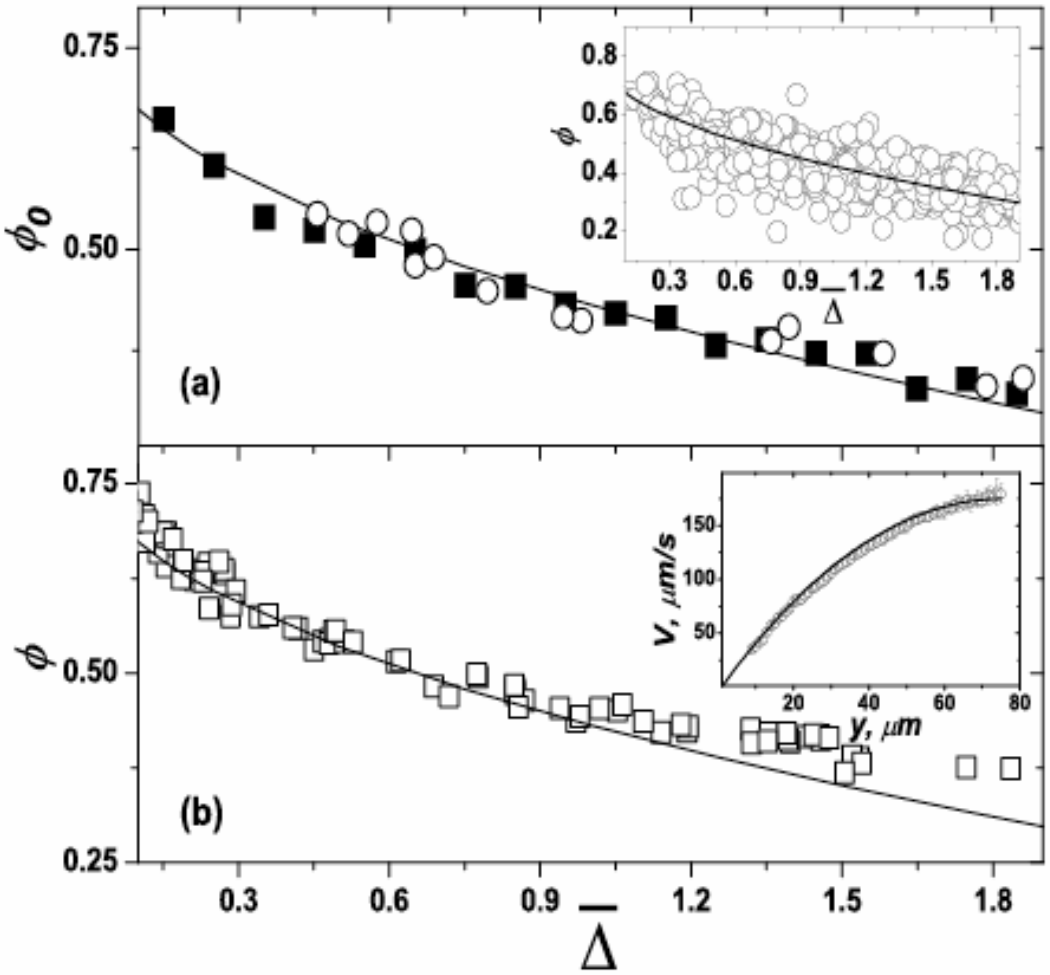

$$\phi_0 = \frac{1}{2}\arctan\left(\frac{a-\overline{\Delta}}{\overline{\Delta}}\right)^{1/2} \approx \frac{\pi}{4} - \frac{\overline{\Delta}^{1/2}}{2a^{1/2}};$$

$\overline{\Delta}$ -systematic part of the excess area

$$a \approx 1.994$$

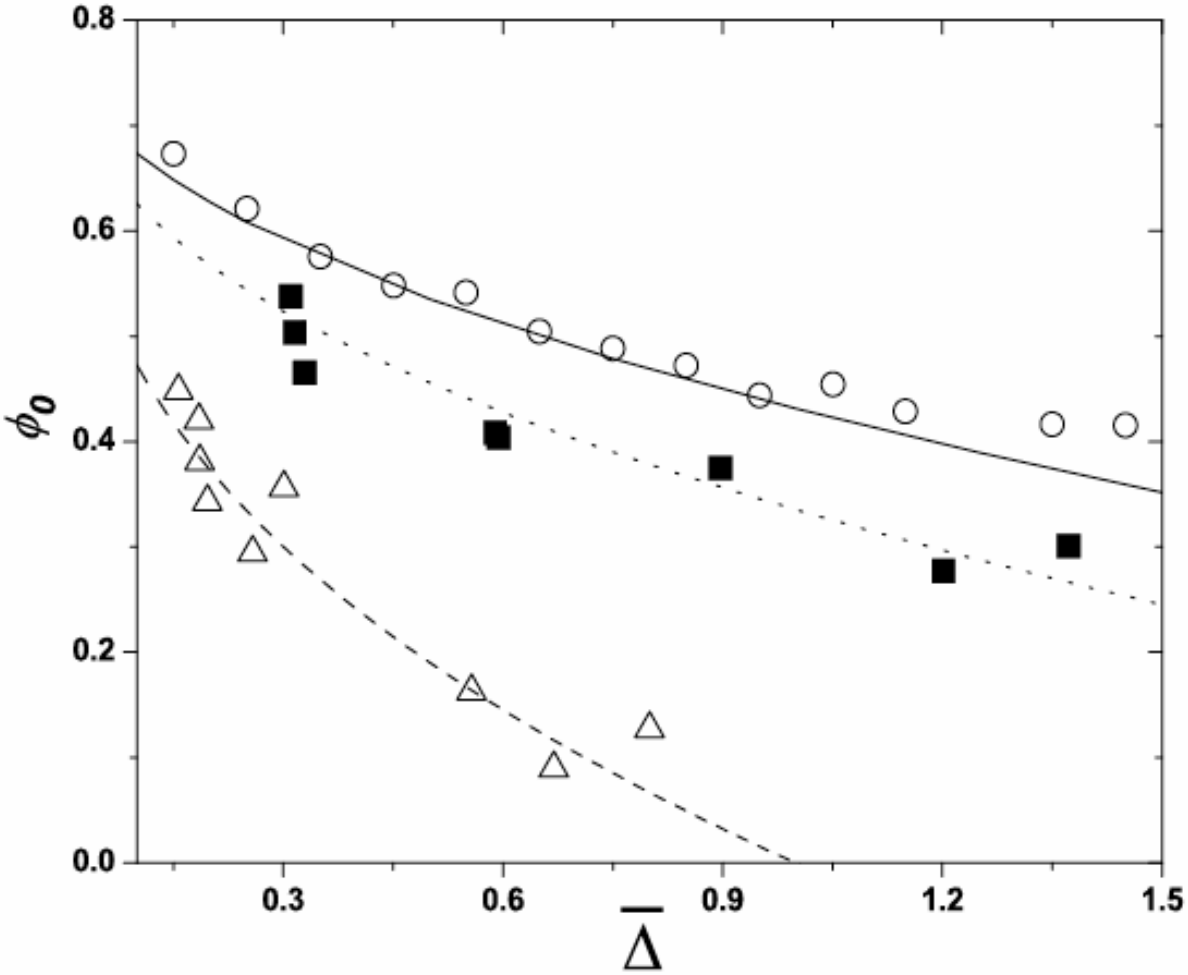

$\varepsilon = 1$ circles

$\varepsilon = 2.7$ squares

$\varepsilon = 5.6$ triangles

$\phi_0 = \pi/4 - \alpha\overline{\Delta}^{\beta}$

$\alpha = 0.785; \beta = 0.4$ dotted curve

$\alpha = 0.45; \beta = 0.45$ dashed curve

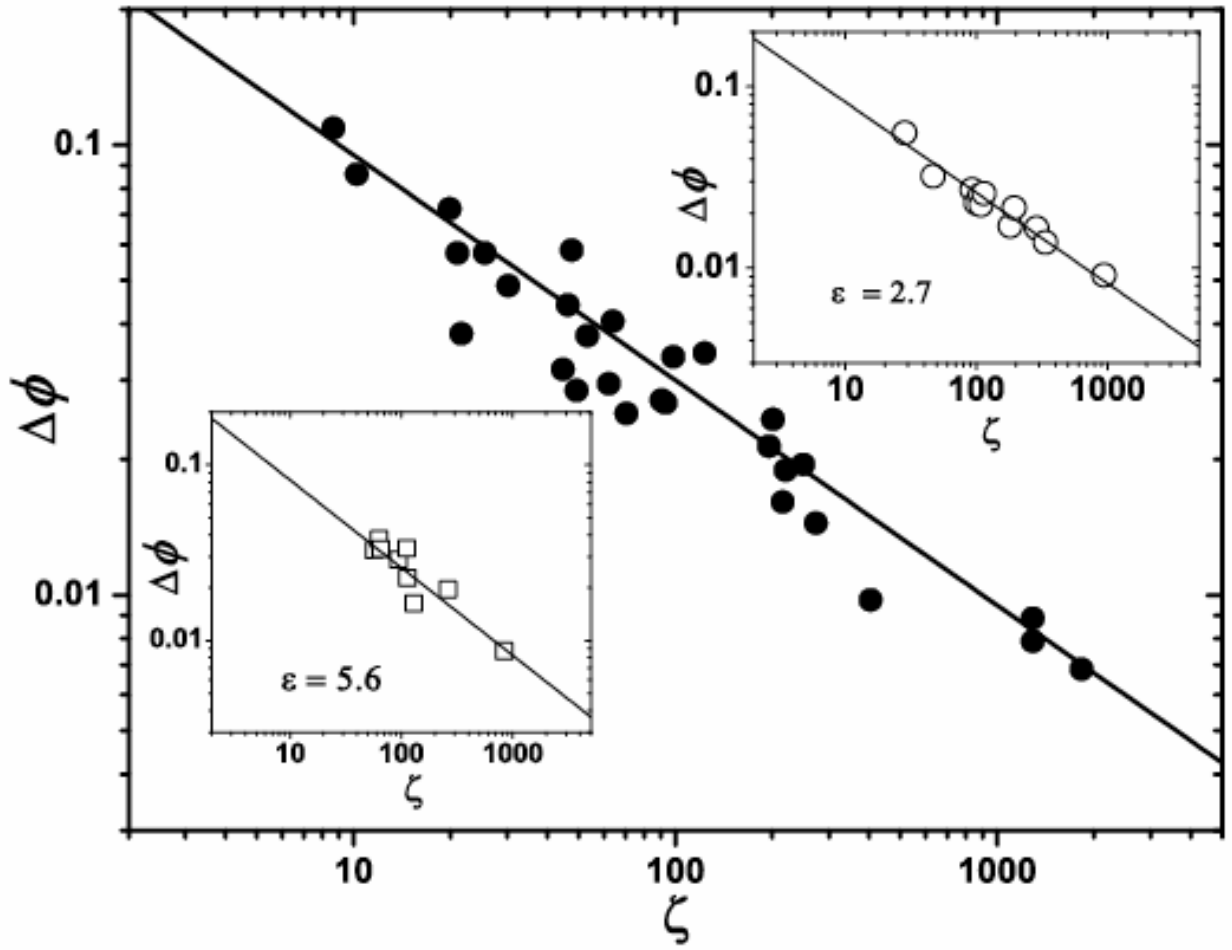

$$\Delta\phi = \left(\frac{24}{55} \frac{1}{4a^{1/2}\varsigma} \right)^{1/2} \cong 0.28\varsigma^{-1/2}$$

$$\varsigma \equiv \chi\kappa\overline{\Delta}^{1/2} / k_B T$$

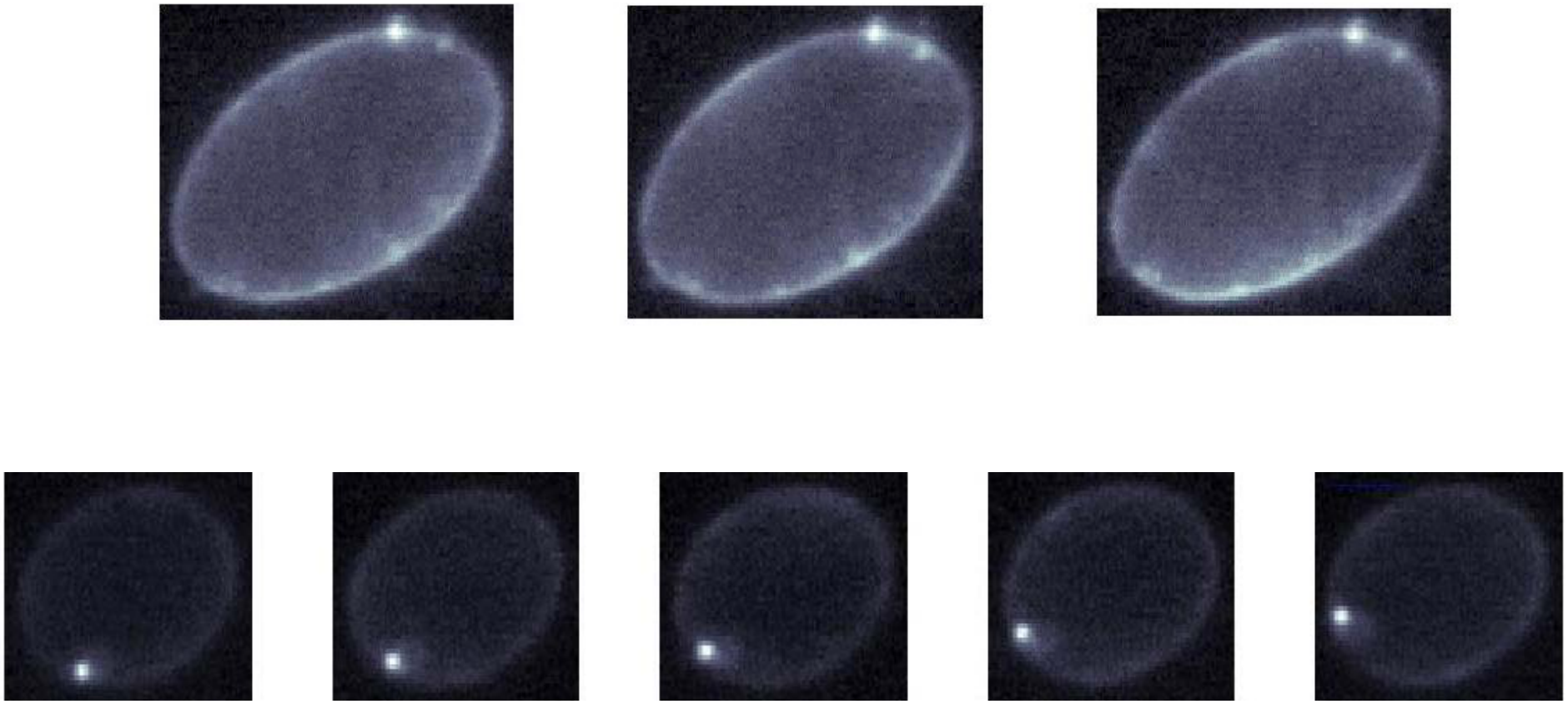

Fluorescent vesicle with fluorescent bead attached by avidin-biotin bonds

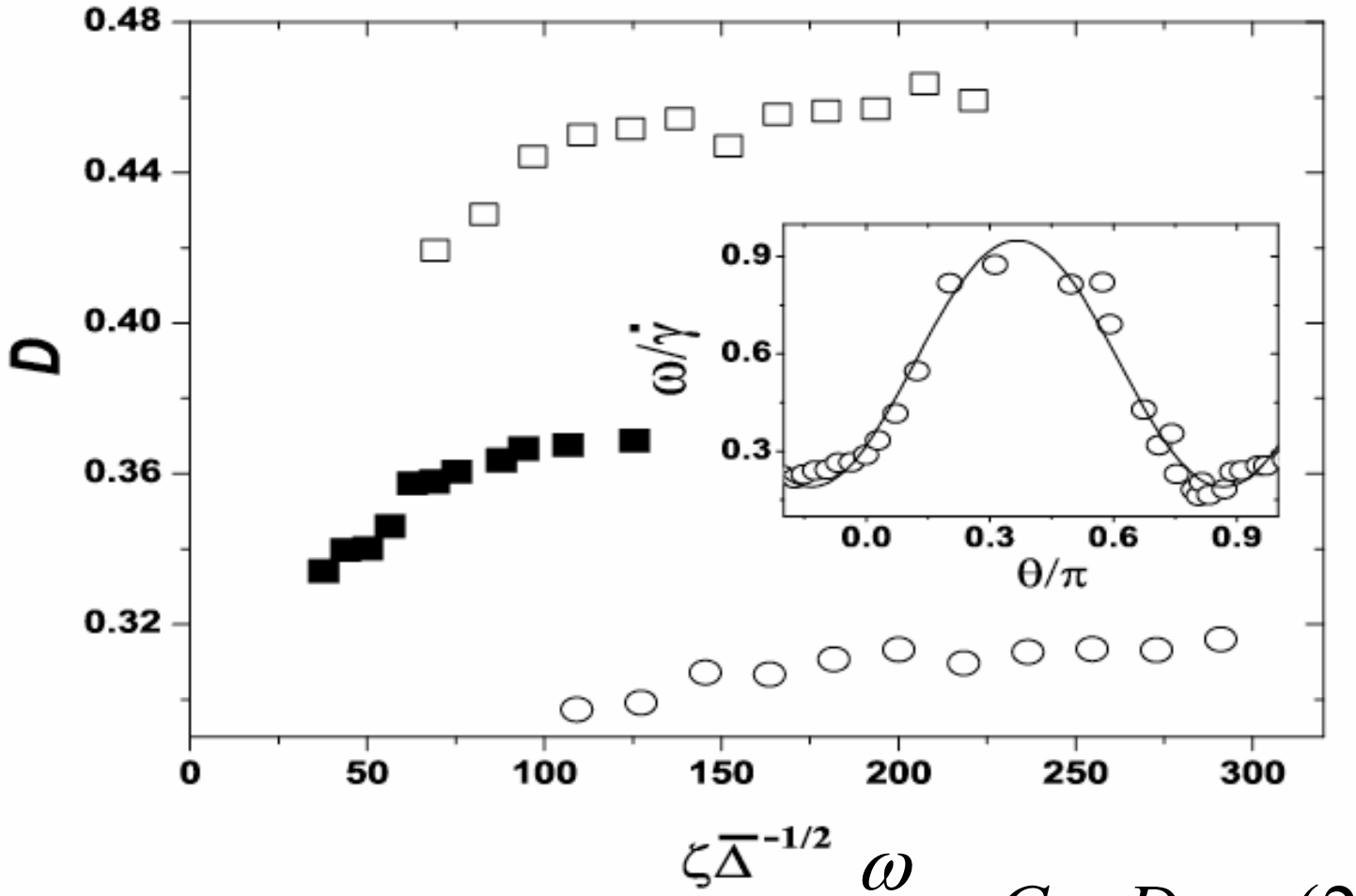

$$D = \frac{L - B}{L + B}$$

$$\frac{\omega}{\dot{\gamma}} = C + D\cos(2\theta)$$

$$C = 0.57; D = 0.38$$

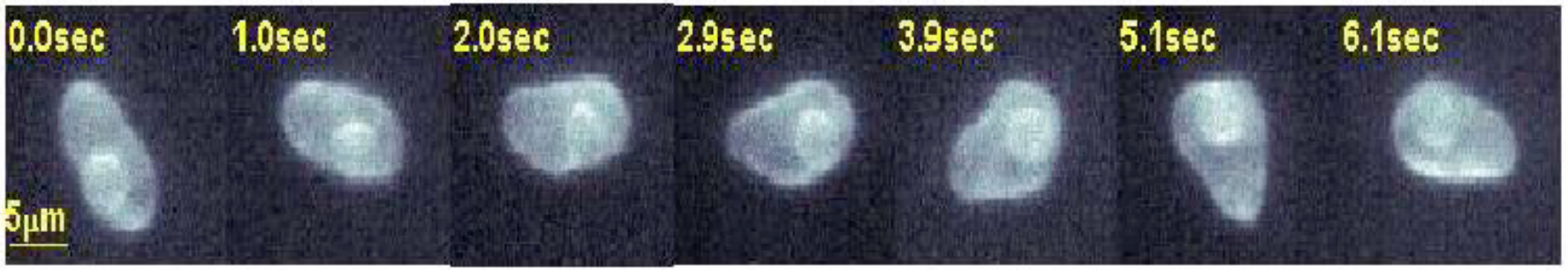
0.0sec
1.0sec
2.0sec
2.9sec
3.9sec
5.1sec
6.1sec
5μm


0.0sec
0.2sec
0.5sec
0.7sec
1.0sec
1.3sec
1.5sec
5μm